Journal of Experimental Botany, Vol. 74, No. 8 pp. 2620–2637, 2023
https://doi.org/10.1093/jxb/erad043 Advance Access Publication 6 March 2023

RESEARCH PAPER

Nutrient availability regulates *Deschampsia antarctica* photosynthetic and stress tolerance performance in Antarctica

Jorge Gago[1,*,†], Miquel Nadal[1,2,†], María José Clemente-Moreno[1], Carlos María Figueroa[3], David Barbosa Medeiros[4], Neus Cubo-Ribas[1], Lohengrin Alexis Cavieres[5,6], Javier Gulías[1], Alisdair Robert Fernie[4], Jaume Flexas[1] and León Aloys Bravo[7]

[1] Research Group on Plant Biology under Mediterranean Conditions, Universitat de les Illes Balears (UIB)/Instituto de Investigaciones Agroambientales y de Economía del Agua (INAGEA), Ctra. Valldemossa km 7.5, 07122 Palma, Spain
[2] Departamento de Sistemas Agrícolas, Forestales y Medio Ambiente, Centro de Investigación y Tecnología Agroalimentaria de Aragón (CITA), Avda. Montañana 930, 50059 Zaragoza, Spain
[3] Instituto de Agrobiotecnología del Litoral, UNL, CONICET, FBCB, 3000 Santa Fe, Argentina
[4] Central Metabolism Group, Molecular Physiology Department, Max-Planck-Institut für Molekulare Pflanzenphysiologie, Golm, Germany
[5] Departamento de Botánica, Facultad de Ciencias Naturales y Oceanográficas, Universidad de Concepción and Instituto de Ecología y Biodiversidad (IEB), Concepción, Chile
[6] Center of Plant, Soil Interaction and Natural Resources Biotechnology, Scientific and Technological Bioresource Nucleus. Universidad de La Frontera, Temuco, Chile
[7] Laboratorio de Fisiología y Biología Molecular Vegetal, Dpt. de Cs. Agronómicas y Recursos Naturales, Facultad de Cs. Agropecuarias y Forestales, Instituto de Agroindustria, Universidad de La Frontera, Temuco, Chile

[†] These authors contributed equally to this work.
* Correspondence: jorge.gago@uib.es or xurxogago@gmail.com

Received 27 October 2022; Editorial decision 24 January 2023; Accepted 5 March 2023

Editor: Johannes Kromdijk, University of Cambridge, UK

Abstract

***Deschampsia antarctica* is one of the only two native vascular plants in Antarctica, mostly located in the ice-free areas of the Peninsula's coast and adjacent islands. This region is characterized by a short growing season, frequent extreme climatic events, and soils with reduced nutrient availability. However, it is unknown whether its photosynthetic and stress tolerance mechanisms are affected by the availability of nutrients to deal with this particular environment. We studied the photosynthetic, primary metabolic, and stress tolerance performance of *D. antarctica* plants growing on three close sites (<500 m) with contrasting soil nutrient conditions. Plants from all sites showed similar photosynthetic rates, but mesophyll conductance and photobiochemistry were more limiting (~25%) in plants growing on low-nutrient availability soils. Additionally, these plants showed higher stress levels and larger investments in photoprotection and carbon pools, most probably driven by the need to stabilize proteins and membranes, and remodel cell walls. In contrast, when nutrients were readily available, plants shifted their carbon investment towards amino acids related to osmoprotection, growth, antioxidants, and polyamines, leading to vigorous plants without appreciable levels of stress. Taken together, these findings demonstrate that *D. antarctica* displays differential physiological performances to cope with adverse conditions depending on resource availability, allowing it to maximize stress tolerance without jeopardizing photosynthetic capacity.**

Keywords: Mesophyll conductance, nutrient mobilization, photobiochemistry, photosynthetic limitations, polyamines, primary metabolism, stomatal conductance.

Introduction

Maritime Antarctica and the Antarctic Peninsula (AP) are amongst the world regions that have experienced the strongest warming trends during the last part of the 20th century (Turner *et al.*, 2016; Jones *et al.*, 2019). A small fraction of the territory of the AP is free of ice and snow, and only two vascular species have naturally colonized these ice-free habitats: the Antarctic hair grass *Deschampsia antarctica* Desv. (Poaceae) and the Antarctic pearlwort *Colobanthus quitensis* (Kunth) Bartl. (Caryophyllaceae) (Peat *et al.*, 2007).

Climate conditions in the AP, even during the short growing season, are characterized by slightly positive temperatures during the day and frequent sub-zero temperatures during the night, along with strong winds and highly variable solar radiation (Cavieres *et al.*, 2016; Convey *et al.*, 2018). Furthermore, the soils of the AP are characterized by low nutrient availability (Blume *et al.*, 2002; Beyer *et al.*, 2020), imposing an additional stress that plants must deal with in order to survive. Moreover, soil conditions may change over a short distance, in many cases from meter to meter, due to strong influences of cryoturbation and solifluction (Blume *et al.*, 2002) and nutrient enrichments from seabird guano, as well as debris from mosses, lichens, and algae (Campbell and Claridge, 1987; Beyer *et al.*, 1999; Bolter, 2011). Nutrient availability in cold ecosystems strongly depends on soil temperature, soil moisture (SM), and the activity of soil microbiota, which in turn control nitrogen fixation and mineralization, organic matter (OM) decomposition, etc. (Hobbie *et al.*, 2007; Convey *et al.*, 2012; Farrer *et al.*, 2013). In fact, several studies in the Arctic tundra positively relate SM with increased OM decomposition, that would release nutrients to the soil solution (Glanville *et al.*, 2012; Hicks Pries *et al.*, 2013; Scharn *et al.*, 2021), facilitating their availability for the tundra plant's uptake (Schimel *et al.*, 1996; Semenchuk *et al.*, 2015). Considering the observed global warming trends and the expected higher temperatures for the AP as well as water availability, soil nutrient cycles could be altered, with the potential to influence plant productivity (Wasley *et al.*, 2006; Hill *et al.*, 2011, 2019). In this sense, changes in the availability of nutrients in Antarctic soils could alter the ecophysiological performance of the species by affecting the allocation of resources between traits and physiological processes related to productivity, stress tolerance, or reproduction, that could finally lead to changes in abundance and composition of plant communities as has been observed in arctic (Chapin *et al.*, 1996; Hobbie *et al.*, 2007; Peterson, 2014) and alpine tundras (Bowman *et al.*, 1993; Körner, 2021).

Deschampsia antarctica (hereafter DA) is distributed from the Andes of central Argentina and Chile to sub-Antarctic islands and adjacent islands of the AP, spanning diverse soil types with a wide range of nutrient availability (Komárková *et al.*, 1985; Smith, 2003; Androsiuk *et al.*, 2021). Several authors reported that DA populations in the AP showed higher density in soils containing high levels of P and OM, such as those found on the surroundings of penguin rookeries and zones with elevated moss cover, suggesting that soil nutrients are important drivers of DA abundance (Smykla *et al.*, 2007; Park *et al.*, 2012, 2013). Different physiological adaptations to face soil nutrient scarcity have been described in this species; among them, the capacity of incorporating N in the form of free amino acids and short-chain peptides is remarkable (Hill *et al.*, 2011). Also, under controlled conditions, and in terms of biomass production, a larger and faster growth response was described when exposed to NH_4^+ than NO_3^-, probably due to the lower energetic cost related to NH_4^+ assimilation (Rabert *et al.*, 2017).

In any case, in Antarctica, DA needs to obtain a positive carbon balance in an environment characterized by low temperature and limited availability of nutrients. Xiong *et al.* (1999), measuring short-term photosynthetic temperature response curves, described that DA can sustain up to 30% of its assimilation rates at 0 °C. Moreover, DA showed structural and physiological leaf traits typical of species from xeric environments, such as an elevated leaf mass area (LMA), thick cell walls, and a high Rubisco specificity factor (Sáez *et al.*, 2017). Nutrients such as N and P are directly linked with the carbon assimilation capacity (Walker *et al.*, 2014); N is a major and essential element of the whole photosynthetic machinery, from chlorophylls to Rubisco (Evans and Clarke, 2019), while P is involved in ribulose bisphosphate (RuBP) regeneration, production of energy (ATP) and reduction power (NADPH), synthesis of phosphorylated intermediates of the Calvin–Benson cycle (CBC), and regulation of starch and sucrose synthesis (Lambers *et al.*, 2008). Low temperature environments can exacerbate photosynthetic limitations by constraining enzymatic activity (Hurry *et al.*, 2000). Additionally, the reduced nutrient availability of the Antarctic tundra leads to photoinhibition and reduced carbon assimilation (Ensminger *et al.*, 2006).

When photosynthesis (A) is constrained by one or a combination of these environmental factors (i.e. temperature and nutrient availability), it cannot operate as an energy sink, thus driving an increase in reactive oxygen species (ROS) (Fernández-Marín *et al.*, 2020). Under low temperatures and high radiations, DA showed a higher activation of ROS-scavenging mechanisms, such as the water–water cycle, to protect PSII, and higher levels of superoxide dismutase and ascorbate

peroxidase compared with other species from the same family (Pérez-Torres *et al.*, 2004a, b, 2007). DA also displays an elevated antioxidant capacity which, in combination with leaf nutrient mobilization, suggests a trade-off between catabolism and maintenance of leaf functionality under stress (Clemente-Moreno *et al.*, 2020). Additionally, DA displays a high activity of anti-freezing proteins, high levels of sugars (which act as osmoprotectants), and an elevated percentage of unsaturated fatty acids, thus ensuring membrane fluidity and functionality under low temperatures (Bravo *et al.*, 2001).

Despite the knowledge obtained on the physiological characteristics of DA, the answers to the following questions remain elusive. Has DA developed differential photosynthetic and stress tolerance mechanisms based on the availability of nutrients? Is there any link between the photosynthetic capacity and the molecular and physiological mechanisms for coordinating stress tolerance? Which are the molecular and physiological mechanisms driving a positive net carbon balance without jeopardizing survival in one of the most extreme environments for vascular plants on Earth? Understanding these processes will allow us to foretell the performance and putative success of DA under the predicted warming scenarios in maritime Antarctica.

Materials and methods

Experimental sites and environmental conditions

Deschampsia antarctica plants were studied near the Henryk Arctowski Polish Antarctic Station (62°09′S, 58°28′W) in King George Island (KGI) in the South Shetlands (maritime Antarctica) between 5 and 12 February 2018. Three different sites were selected to investigate the plants' performance under different soil nutrient regimes: (i) Puchalski hill (PUCH) (62°09′47.11″S, 58°27′58.15″W), characterized by a complete vegetation cover dominated by lichens and mosses, such as *Sanionia georgicouncinata*, *Polytrichum piliferum*, and *Polytrichastrum alpinum* (Kozeretska *et al.*, 2010), where DA grows associated with the moss carpet created by these species (Casanova-Katny and Cavieres, 2012; Cavieres *et al.*, 2018); (ii) the surroundings of a penguin colony (PINGU) (62°09′44.46″S, 58°27′45.15″W), with soil affected by significant penguin droppings, close to the seashore, characterized by gravel and rocks covered by lichens; and (iii) within the Henryk Arctowski station area (BASE), under a human-altered environment, with no homogeneous plant community established, and usual presence of different birds and marine mammals employing this area as a resting site (62°09′37.32″S, 58°28′23.83″W). It is important to note that distances between these sites and the base station are <500 m, and that the individuals were not sheltered and thus shared the climatological conditions prevailing in the area. Plants at PUCH showed small leaves with a mixed pattern of greenish and yellowish leaves, indicating different degrees of leaf senescence within the same individual. However, at PINGU and BASE sites, DA plants were much more vigorous and with a green, homogeneous pattern for all leaves (Fig. 1).

From December 2017 to February 2018, the mean air temperature at PUCH was ~6.9 °C (with an absolute minimum of −4.1 °C in December 2017, and maximum of 16.6 °C in February 2018) (Supplementary Fig. S1). Year-round precipitation falls mostly as snow (~700 mm), and summer days are usually windy and cloudy, although for short periods clear skies produce high irradiance incidences of ~2000 μmol m^{-2} s^{-1} (Angiel *et al.*, 2010).

Soil characterization

Soil samples were collected at each of the three study sites (three plots per site, 3 × 3 m each), with three independent subsamples per plot in the vicinity of the plant population. The top-soil layer (5–7 cm) was manually removed, and samples were taken from the top 7–15 cm of soil at each plot. The three independent samples were obtained by mixing three subsamples (300 g each) randomly collected within each plot (avoiding large rocks and gravel outcrops) with DA individuals being between 10 cm and 50 cm distant from soil subsampling. After the removal of plant and root remains from the soil samples, they were passed through a 2 mm sieve and dried in the oven at 62 °C up to constant weight.

N and P contents were determined by the Kjeldahl and Mehlich methods, respectively (Mehlich, 1984). The content of exchangeable cations [cation exchange capacity (CEC) for Ca^{2+}, Mg^{2+}, K^{+}, and Na^{+}] was analyzed after extraction with ammonium acetate (Metson, 1956). pH, electric conductivity, and OM content were measured following previous protocols (Chapman and Pratt, 1962; Bower and Wilcox, 1965). All the analyses were performed by the soil analysis service of the Agricultural Council of the Balearic Islands Government.

The SM at each site was assessed as volumetric water content measured next to the sampled plants using a humidity probe (WET-2 Sensor/HH2 Moisture Meter, Delta-T Devices, Cambridge, UK).

The three study sites presented a similar texture and can be classified as sandy soils (Supplementary Table S1); in contrast, soil fertility parameters of the three sites significantly differed. While all the samples showed an extremely high exchangeable sodium percentage (ESP; >50%), the soil from PUCH was characterized by low pH (5.15) and electric conductivity (0.12 dS m^{-1}), with moderate OM content (2.75%) and CEC (3.58 mEq/100 g), compared with the other two sites. The soil from PINGU also showed low pH (5.09) but higher electric conductivity (0.49 dS m^{-1}) and OM content (6.26%) than PUCH; conversely, the CEC from PINGU was slightly lower (3.37 mEq/100 g) than that from PUCH. On the other hand, the soil from BASE presented higher pH (6.27) and CEC (4.78 mEq/100 g) than the other two sampling sites, a very low OM content (0.62%), and intermediate electric conductivity (0.21 dS m^{-1}). The differences in CEC among sites were mainly due to Ca^{2+} and Mg^{2+}, which were significantly higher at BASE, and to K^{+}, which was significantly lower at PUCH than at the other two sites. The soil from PINGU showed the highest contents of N and P, as well as the micronutrient Cu, while BASE soils displayed higher levels of Mn and Zn than the other two sites (Supplementary Table S1). A complete characterization of the soil total element content is presented in Supplementary Table S2, which shows that other elements (such as S, Si, and Mo) displayed higher values at PINGU than at PUCH and BASE. Regarding the SM measurements, PINGU showed significantly higher values than PUCH, whereas BASE presented intermediate values between the other two sites (Supplementary Table S1).

Leaf ionomics, leaf mass per area, and dry matter content

Leaf samples (8–9 biological replicates per site) and soil samples (as described in the previous section) were obtained to analyze the major elements (B, C, Ca, Cu, Fe, K, Mg, Mn, Mo, N, Na, P, S, Tl, and Zn). Approximately, 300 mg FW of completely expanded leaves were sampled per individual. Measurements were carried out in an ICP THERMO ICAP 6500 DUO spectrometer (Thermo Scientific). C and N total contents were analyzed by combustion at 950 °C coupled to individual infrared detection and thermal conductivity. These analyses were performed in the CEBAS-CSIC Ionomic Service in Murcia, Spain. Prior to the element analysis, additional leaves (eight biological replicates per site, the same as those employed for gas exchange and chlorophyll fluorescence analysis) were used to determine the fresh and dry weight to calculate the leaf dry matter content (LDMC), as the ratio between fresh and dry weight, following the recommendations of Vaieretti *et al.* (2007).

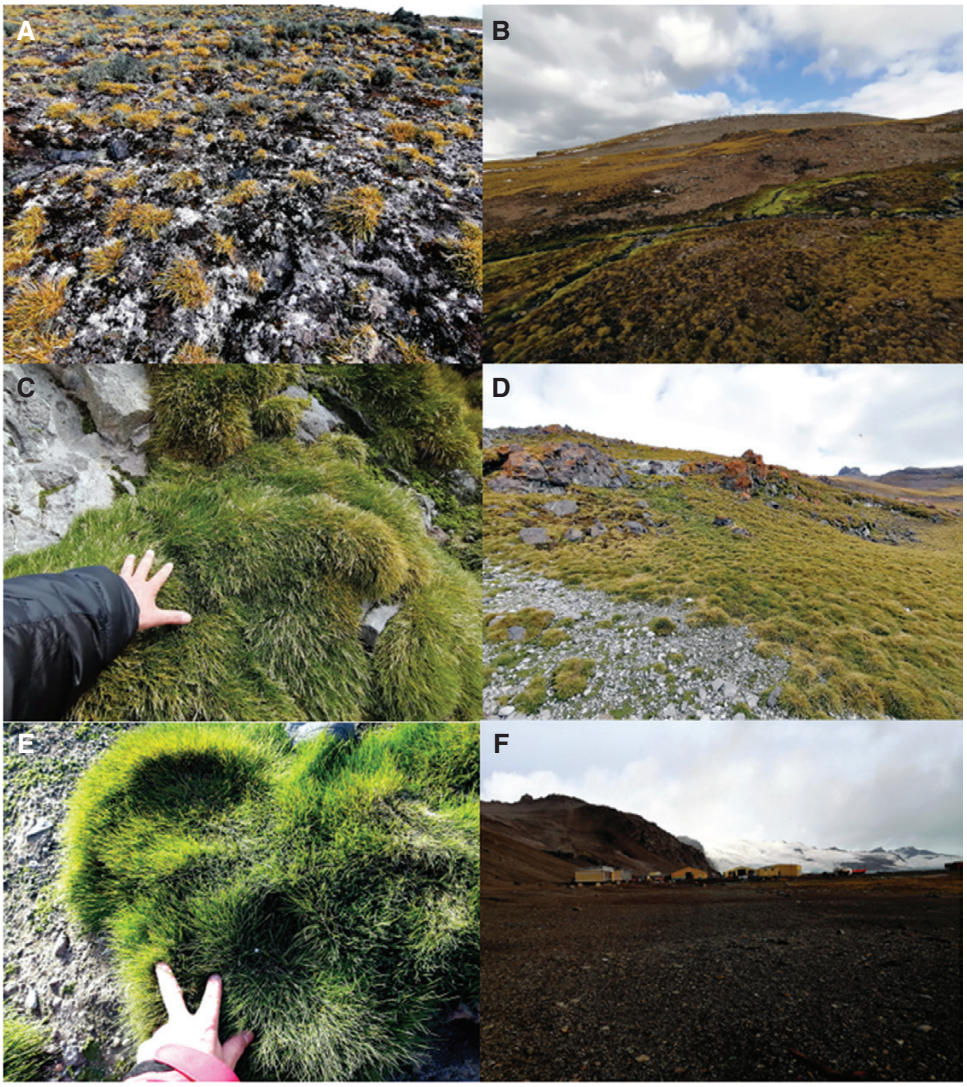

Fig. 1. Selected locations for the analysis of *Deschampsia antarctica* (DA) plants. (A) DA growing between mosses and lichens at the top of Puchalski hill (B), (C) DA growing in the vicinity of the penguin rookeries (D), and (E) DA individuals growing in the surroundings of the Henryk Arctowski Research Polish Station (F) at King George Island (South Shetland, maritime Antarctica). We thank Dr Melanie Morales for kindly providing us with the images.

The LMA was calculated as the ratio between the leaf area (measured in fresh leaves using the Image J software; https://imagej.nih.gov/ij/index.html) and the dry weight of the same leaves (obtained after drying at 80 °C for 72 h).

Gas exchange and chlorophyll fluorescence

Plants from the three study sites were collected in the field during the early morning from each location for same-day measurements. Turfs with individuals were carefully removed from the ground, ensuring enough soil was kept to minimize root damage, air exposure, or water stress, and transported to the vicinity of the lab's station for subsequent photosynthesis measurements.

Leaf photosynthesis measurements were conducted on eight different individuals per experimental site using an open gas exchange system with a fluorometer (Li-6400XT; Li-Cor Inc., Lincoln, NE, USA) employing a fluorescence chamber of 2 cm^2 (Li-6400-40). Leaves were carefully placed in the equipment measurement chamber, avoiding overlaps between them, and ensuring contact with the leaf thermocouple. When leaves did not cover the full chamber, a picture of the leaves inside the chamber's foam gasket was taken to subsequently re-calculate the area with the image software Image J. This area was later employed for the final gas exchange calculations. CO_2 leakage in the gasket–sample interface was corrected following Flexas *et al.* (2007). The block temperature was set to 15 °C for all measurements, in order to work at the plant's optimal photosynthetic temperature (Edwards and Smith, 1988; Xiong *et al.*, 1999; Sáez *et al.*, 2017; Clemente-Moreno *et al.*, 2020).

Light response curves were performed at a CO_2 atmospheric concentration (C_a) of 400 ppm and light intensities from 0 to 2000 µmol photons m^{-2} s^{-1} through nine consecutive steps (2–3 min per step: 0, 50, 100, 300, 500, 900, 1200, 1500, and 2000 µmol photons m^{-2} s^{-1}) to determine the saturating photosynthetic photon flux density (PPFD) for subsequent measurements (determined as 1200 µmol photons m^{-2} s^{-1}), as previously observed in Sáez *et al.* (2017) and Clemente-Moreno *et al.* (2020).

Instantaneous measurements of light-saturated net CO_2 assimilation (A_{area}), stomatal conductance to CO_2 diffusion (g_{sc}), substomatal CO_2 concentration (C_i), maximum fluorescence in the light under a saturating

pulse (F_m'; measuring beam intensity 1 µmol m^{-2} s^{-1}, 8000 µmol quanta m^{-2} s^{-1}, 0.8 s duration), and steady-state yield of fluorescence in the light (F_t) were recorded 20–30 min after clamping.

Leaf chamber conditions were maintained at 400 ppm of C_a, 1200 µmol m^{-2} s^{-1} of PPFD (90:10% red:blue light), 50–70% relative humidity, and 15 °C block temperature, as in Clemente-Moreno *et al.* (2020). Afterwards, CO_2 response curves (A–C_i curves) were performed by subjecting the plants to step-by-step changes in C_a (3–4 min each) as follows: 400, 300, 200, 100, 400, 400, 500, 600, 700, 800, 1250, 1500, and 400 µmol CO_2 mol^{-1} air. The initial measurement at 400 ppm was employed as reference to compare with the same C_a level steps (within and at the end of the curve), in order to ensure that CO_2 changes did not affect the initial photosynthetic steady state. Finally, leaves were kept for 30 min in darkness to record the CO_2 respiration rate (R_d), dark-adapted fluorescence (F'_m), and maximum fluorescence under a saturating pulse (F_m). Mitochondrial respiration in the light was considered as half of R_d (Niinemets *et al.*, 2005; Gallé *et al.*, 2011).

Non-photochemical quenching (NPQ), the maximum quantum yield of PSII (F_v/F_m), and the quantum yield of PSII (Φ_{PSII}) were calculated as described in Maxwell and Johnson (2000). From the instantaneous measurements, the electron transport rate (ETR) was calculated as ETR=Φ_{PSII}×PPFD×αβ (Genty *et al.*, 1989), where αβ is the product of leaf absorptance (α) and the electron partitioning between PSI and PSII (β). The value of α for DA plants from the same location measured by Sáez *et al.* (2017) was used for all measurements performed in this work, and β was assumed to be 0.5 (Pons *et al.*, 2009). The photorespiratory rate (P_r) was estimated combining gas exchange and chlorophyll fluorescence (Valentini *et al.*, 1995). The model assumed that all the reducing power generated by the electron transport chain is employed for photosynthesis and photorespiration, and that chlorophyll fluorescence gives a reliable estimate of quantum yield of electron transport. According to the known stoichiometries of electron use in photorespiration, it can be solved as follows: P_r=1/12 [ETR–4 (A_{area}+R_d/2)]. Mesophyll conductance to CO_2 diffusion (g_m) was estimated using the variable J method ($g_{m\text{-}VJ}$), as $g_{m\text{-}VJ}=A_{area}/\{C_i-\Gamma^\star$ [ETR+8 (A_{area}+R_d/2)]/[ETR–4 (A_{area}+R_d/2)]} (Harley *et al.*, 1992; Pons *et al.*, 2009), where $\Gamma^\star$ is the CO_2 compensation point in the absence of mitochondrial respiration, which was obtained from the Rubisco kinetics at 15 °C measured in Sáez *et al.* (2017) for DA. The CO_2 concentration inside chloroplasts (C_c) was calculated as $C_c=C_i-A_{area}/g_m$. Additionally, mesophyll conductance was estimated from the A–C_i curves using the curve-fitting method ($g_{m\text{-}CF}$) with the Excel Tool provided in Sharkey (2016), from which the C_c-based maximum velocity of Rubisco carboxylation (V_{cmax}) and the maximum electron rate (J_{max}) were also obtained. The Michaelis–Menten constants of Rubisco carboxylation/oxygenation for A–C_i analysis were obtained from Sáez *et al.* (2017). From the A–C_i curve-derived parameters, photosynthetic limitations were estimated following Grassi and Magnani (2005), including the stomatal (l_s), mesophyll (l_m), and biochemical (l_b) relative limitations, and the contributions of stomata (SL), mesophyll (ML), and biochemistry (BL) to dA_{area}/A_{area}, considering the mean A_{area} value from the 'BASE' plants as reference. The product A_{area}/C_c at C_a=400 µmol mol^{-1} was used as a proxy for $\partial A/\partial C_c$. Area-based A_{area} was converted to mass-based assimilation rate (A_{mass}) using LMA from the same individual.

Pigment content analysis and primary metabolism profiling

Leaf samples (from 7–8 different individuals) for pigment and metabolism analysis were collected at midday at the different sites, immediately frozen in liquid nitrogen, and stored at –80 °C.

Pigments were extracted from 100 mg of leaf material powdered with liquid nitrogen using a mortar and pestle. A spatula tip of $CaCO_3$ was added before extracting with 1 ml of 100% HPLC-grade acetone. Pigments were separated and quantified by reversed-phase HPLC. The HPLC system, chromatographic conditions, and quantification of individual pigments were exactly the same as described by Sáez *et al.* (2013).

Metabolite extraction for GC-MS was carried out as previously described (Lisec *et al.*, 2006), using 50 mg of leaf fresh material. Ribitol (0.2 mg ml^{-1} in H_2O) was added during extraction as an internal standard. A dry aliquot (150 µl of the polar phase) was re-suspended in methoxyamine hydrochloride (20 mg ml^{-1} in pyridine) and derivatized using *N*-methyl-*N*-[trimethylsilyl]trifluoroacetamide (MSTFA). The GC-TOF-MS system comprises a CTC CombiPAL autosampler, an Agilent 6890N gas chromatograph, and a LECO Pegasus III TOF-MS running in EI+ mode. A volume of 1 µl of derivatized metabolite solution was used for injection. Peaks were annotated to metabolites by comparing mass spectra and GC retention times with database entries and those of authentic standards available in a reference library from the Golm Metabolome Database (Kopka *et al.*, 2005), using Xcalibur® 2.1 software (Thermo Fisher Scientific).

Data analyses

One-way ANOVA and multiple comparisons Tukey's HSD test (P<0.05) were employed when data fulfilled the normality and homogeneous variance criteria; otherwise, we used the Kruskal–Wallis analysis with Bonferroni post-hoc comparisons (P<0.05) employing the 'dplyr', 'dlookr', 'writexl', and 'agricolae' packages in R software (v. 4.1.1). We also employed the on-line software platform MetaboAnalyst 5.0 (https://www.metaboanalyst.ca) for multivariate analysis and figure plotting of the primary metabolism data. To evaluate the ionomic and primary metabolic profile of the different groups, we used a sparse partial least squares-discriminant analysis (sPLS-DA) to obtain the most important features per component in order to identify the most relevant loadings for each group.

Results

Leaf ion contents show major differences between the studied sites

We analyzed 18 macro- and micronutrients on the leaves of plants from each site (Supplementary Table S3) and, according to the multivariate sPLS-DA considering all the elements, the two major components explained almost 55% of the variance between sites (Fig. 2). PUCH plants were grouped along positive values of principal component 1 (PC1), while the other two groups (PINGU and BASE plants) were located along negative values on this axis, but separated along PC2 (Fig. 2). The mineral elements with higher loading values for PC1 were N, S, Rb, Zn, K, and P, which separated BASE and PINGU (high contents) from PUCH (low contents) (Supplementary Fig. S2). PC2 basically differentiated BASE from PINGU, while PUCH showed an intermediate position; the most relevant mineral elements for PC2 were Pb, Sr, Mo, Ca, Tl, and B.

Comparisons of the leaf element concentrations between sites (Fig. 3; Supplementary Table S3) showed that the C content was slightly lower in PUCH than in BASE, while PINGU showed intermediate levels. Conversely, BASE and PINGU plants showed significantly higher levels of N, P, K, S, and Zn than PUCH (between 1.7- and 4.3-fold). Other mineral elements such as Fe and Mn (more soluble in acidic soils than the previously mentioned elements) did not show statistical differences between sites (Fig. 3).

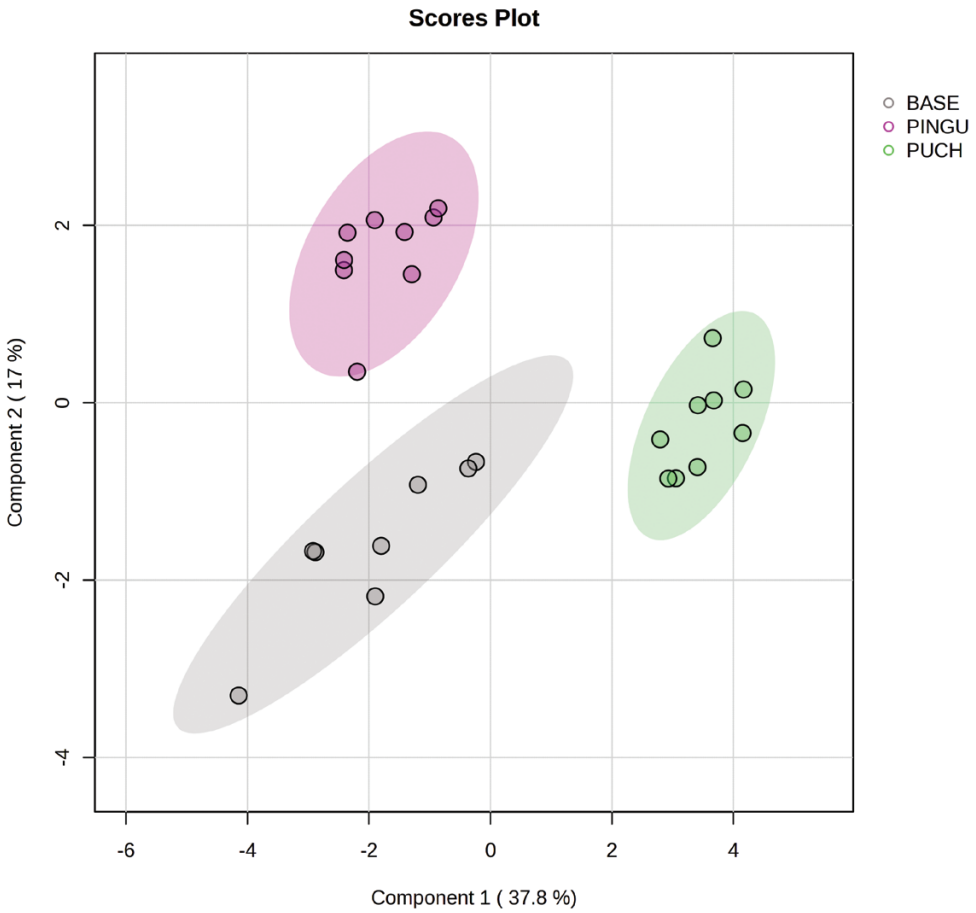

Fig. 2. Sparse partial least square discriminant analysis (sPLS-DA) of the leaf ionomic profile for the plants of the three sites studied in this work: PUCH (tundra site), PINGU (vicinity of the penguin rookeries), and BASE (within the base station).

Nutrient availability affects photosynthetic rates driven by mesophyll conductance and photobiochemistry

The main leaf structural, photosynthetic, and chlorophyll fluorescence parameters are shown in Table 1. There were significant differences between sites for LMA (P=0.01), with PINGU plants showing lower values than plants from the other sites (Table 1), and for LDMC (P<0.001), with PUCH plants showing values ~40% higher than plants from the other two sites. At the photosynthetic level, no differences were observed in the plants between sites on an area basis (A_{area}, P=0.1); meanwhile marginally significant differences were observed on a mass basis (A_{mass}, P=0.09). Also, no differences in g_{sc}, C_i, C_c, and intrinsic water use efficiency (WUE_i) were observed (Table 1). Significant differences were observed for ETR (P<0.001), V_{cmax} and J_{max} (P=0.03 for both), but also for $g_{m\text{-}VJ}$ (P=0.04), where BASE and PINGU plants showed higher values than PUCH plants (Table 1). The maximum photochemical quantum efficiency of the PSII (F_v/F_m), a common stress physiological indicator, also showed differences between sites (P<0.001), where PUCH plants obtained significantly lower values (Table 1).

We further explored the relationship between A_{area} and its physiological and biochemical drivers g_{sc}, $g_{m\text{-}VJ}$, ETR, V_{cmax}, and J_{max} (Supplementary Fig. S3). The relationship between A_{area} and g_{sc} showed a positive saturation curve up to 0.15 mol CO_2 m^{-2} s^{-1} (polynomial regression P<0.001, Supplementary Fig. S3A). Conversely, linear positive correlations were observed for g_m (P<0.001, Supplementary Fig. S3B) and for ETR, V_{cmax}, and J_{max} (Supplementary Fig. S3C–E). Altogether, these data indicated that the highest A_{area} values were associated with higher g_m and photobiochemistry for BASE and PINGU plants, rather than elevated g_{sc} values.

The assumptions performed to estimate g_m were tested employing two independent and different methodologies, the curve-fitting method (Sharkey *et al.*, 2007) and the variable J method (Harley *et al.*, 1992). The relationship between both estimations showed a significant agreement (R^2=0.67,

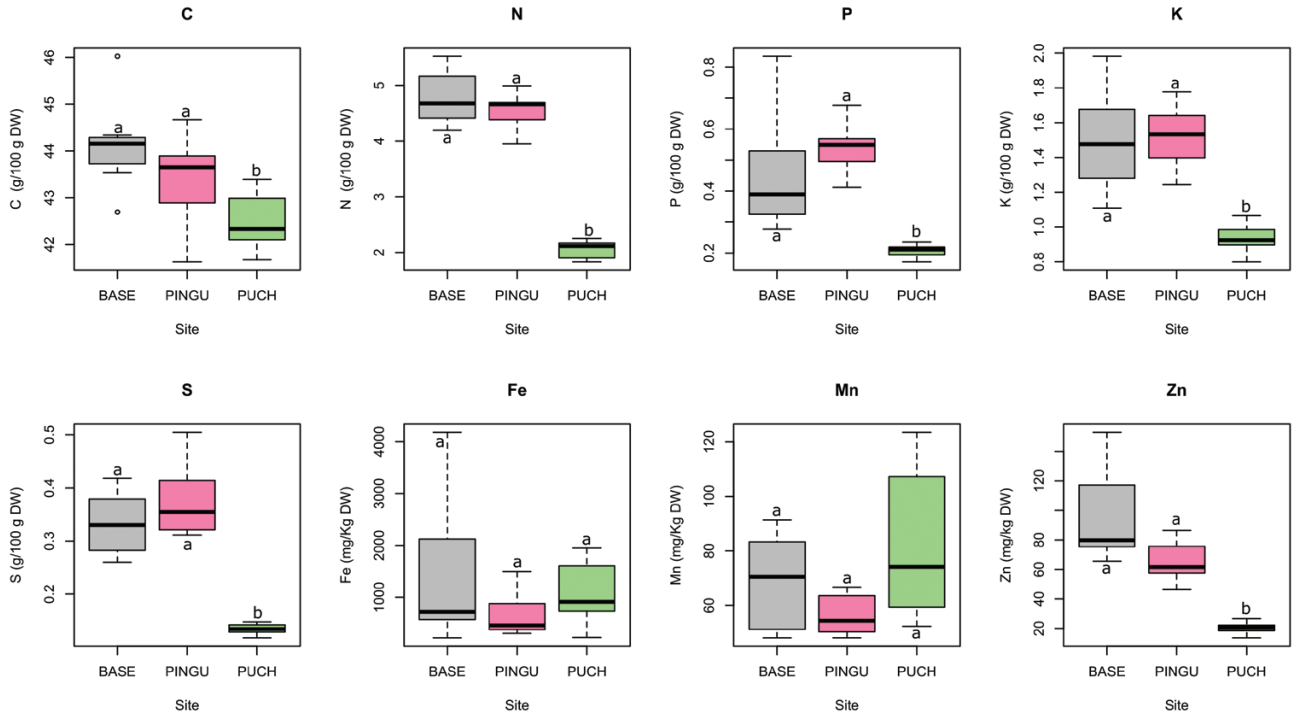

Fig. 3. Leaf element content of macro- and micronutrients that showed major differences between the three different sites: BASE (within the base station), PINGU (vicinity of the penguin rookeries), and PUCH (tundra site). Site effect was evaluated by one-way ANOVA, and different letters indicate statistical differences by Tukey's HSD test (P<0.05).

P<0.001; Supplementary Fig. S4). The photosynthetic response to CO_2 on a C_c basis, where BASE plants showed the highest A_{area} values, was closely followed by plants from PINGU, while PUCH plants showed the lowest values (Supplementary Fig. S5). In fact, V_{cmax} and J_{max} calculations showed that PUCH plants had significantly lower values, PINGU showed an intermediate position between the other two sites, and BASE displayed the highest values for these parameters (Supplementary Fig. S5; Table 1).

We performed a limitation analysis (Grassi and Magnani, 2005) to explore the diffusive and biochemical drivers of A_{area}, and to quantify the relative photosynthetic limitations in plants from different sites. There were no significant differences between BASE and PINGU plants, but plants from PUCH showed significant limitations by mesophyll conductance and photobiochemistry to their photosynthetic capacity compared with BASE and, to a lesser extent, PINGU plants (Table 2).

DA plants in BASE and PINGU sites did not show reductions in the physiological stress indicator F_v/F_m; however, the F_v/F_m was significantly lower in PUCH plants (Table 1). Changes in the F_v/F_m performance were not accompanied by correlative changes in the NPQ (Supplementary Table S4), commonly associated with photoprotection and VAZ cycle activation. Similarly, F_v/F_m did not relate to a structural leaf trait such as as LMA, but it was significantly and positively correlated to A_{area} (P<0.01), A_{mass} (P=0.017), ETR (P<0.001), P_r (P=0.015), g_{sc} (P=0.046), $g_{m\text{-}CF}$ (P=0.024), V_{cmax} (P=0.01), and J_{max} (P=0.001) (Supplementary Table S4). Altogether, these results additionally indicated that the stress status (reflected by F_v/F_m) was highly related to the plants' gas exchange performance.

Photosynthetic pigment profile

Characterization of photosynthetic pigments is relevant to understand macro- and micronutrient investments (such as N, Fe, and Mg), as well as light harvesting capacities and photoprotection. Significant site effects were detected by ANOVA for the following pigments: Chl *a* and *b* (P=0.03), neoxanthin (P=0.02), violaxanthin (P=0.003), zeaxanthin (P=0.02), and the sum of violoxanthin and anteraxanthin (VA, P=0.02). In general, plants from PUCH showed significantly lower contents of these pigments compared with BASE plants, while PINGU plants presented intermediate values (Table 3).

We also calculated the ratios between Chl *a* and *b*, the AZ:VAZ of the xanthophyll cycle, xanthophylls and carotenes normalized per total chlorophyll, and the de-epoxidation state (Table 4). In this case, the ANOVA showed significant site differences for all parameters except for the Neo/Chl ratio. PUCH plants showed significant higher values for the Chl *a*/*b* ratio, (AZ)/VAZ, β-carotenes versus the total chlorophyll ratio (B-car/Chl), VAZ/Chl, A/Chl, and Z/Chl compared with BASE plants (Table 4). Interestingly, plants from PINGU

Table 1. Structural and photosynthetic parameters measured in the different sites

Site	BASE	PINGU	PUCH	*F*	*P*-value
LMA ($g\ m^{-2}$)	47.44 ± 2.75 a	37.92 ± 1.16 b	45.59 ± 2.26 ab	54.599	0.012*
LDMC	0.27 ± 0.003 a	0.270 ± 0.008 a	0.380 ± 0.010 b	71.665	<0.001***
A_{area} ($\mu mol\ m^{-2}\ s^{-1}$)	13.29 ± 0.75 a	11.48 ± 1.48 a	9.83 ± 0.88 a	25.363	0.103
A_{mass} ($nmol\ g^{-1}\ s^{-1}$)	286.58 ± 23.85 a	307.84 ± 42.19 a	216.13 ± 17.05 a	26.193	0.096
ETR ($\mu mol\ m^{-2}\ s^{-1}$)	159.42 ± 7.62 a	131.8 ± 7.94 b	121.18 ± 6.29 b	72.705	0.004**
P_r ($\mu mol\ m^{-2}\ s^{-1}$)	8.49 ± 0.58 a	6.86 ± 0.46 a	6.64 ± 0.58 a	34.345	0.051
g_{sc} ($mol\ m^{-2}\ s^{-1}$)	0.092 ± 0.008 a	0.111 ± 0.022 a	0.083 ± 0.009 a	0.9565	0.400
C_i ($\mu mol\ mol^{-1}$)	237.06 ± 8.92 a	263.43 ± 15.92 a	263.56 ± 11.74 a	14.849	0.249
WUE_i ($\mu mol\ mol^{-1}$)	90.88 ± 5.4 a	76.78 ± 9.94 a	78.15 ± 7.11 a	10.154	0.379
$g_{m\text{-}VJ}$ ($mol\ m^{-2}\ s^{-1}$)	0.081 ± 0.007 a	0.062 ± 0.01 ab	0.051 ± 0.006 b	36.375	0.044*
C_c ($\mu mol\ mol^{-1}$)	68.26 ± 3.78 a	70.95 ± 6.91 a	66.89 ± 6.31 a	0.1261	0.882
V_{cmax} ($\mu mol\ m^{-2}\ s^{-1}$)	71.37 ± 8.98 a	59.41 ± 8.86 ab	40.66 ± 4.89 b	39.279	0.035*
J_{max} ($\mu mol\ m^{-2}\ s^{-1}$)	119.73 ± 5.89 a	105.88 ± 9.87 ab	87.77 ± 7.7 b	40.257	0.033*
R_d ($\mu mol\ m^{-2}\ s^{-1}$)	2.2 ± 0.46 a	1.79 ± 0.37 a	1.38 ± 0.37 a	10.386	0.371
F_v/F_m	0.77 ± 0.01 a	0.75 ± 0.01 a	0.72 ± 0.01 b	11.283	<0.001***
NPQ	1.72 ± 0.15 a	1.93 ± 0.12 a	1.66 ± 0.07 a	12.781	0.300

Mean ±SE (n=8) of leaf mass per area (LMA), leaf dry matter content (LDMC), area- and mass-based net CO_2 assimilation (A_{area} and A_{mass}, respectively), electron transport rate (ETR), photorespiration (P_r), stomatal conductance for CO_2 diffusion (g_{sc}), substomatal CO_2 concentration (C_i), intrinsic water use efficiency (WUE_i), mesophyll conductance to CO_2 diffusion estimated using the variable J ($g_{m\text{-}VJ}$), CO_2 concentration inside chloroplasts (C_c), maximum velocity of Rubisco carboxylation (V_{cmax}) and maximum electron transport rate (J_{max}) estimated using Cc, respiration in the dark (R_d), maximum quantum yield of PSII (F_v/F_m), and non-photochemical quenching (NPQ). Differences among sites (letters) assessed using one-way ANOVA and Tukey's HSD test; P-value: <0.001***, <0.01**, <0.05*.

Table 2. Photosynthetical limitation analysis of *Deschampsia antarctica* plants at each of the three sites studied following Grassi and Magnani (2005)

Site	SL	ML	BL
	(%)	(%)	(%)
BASE	0 a	0 b	0 b
PINGU	–0.2 ± 7.0 a	13.1 ± 6.3 ab	3.2 ± 0.8 ab
PUCH	5.0 ± 4.3 a	19.3 ± 4.3 a	4.3 ± 1.1 a
F	0.295	34.626	51.618
***P*-value**	0.747	0.050	0.015*

Mean ± SE (n=8) of stomatal (SL), mesophyll (ML), and biochemical (BL) contributions to dA/A, considering the 'BASE' group as reference (maximum A_{area}). g_m from curve fitting was used in all cases and $A_{area}/C_{c\text{-}CF}$ at C_a=400 µmol mol^{-1} was used to estimate $\partial A_{area}/\partial C_c$. Differences among sites (letters) assessed using one-way ANOVA and Tukey's HSD test; P-value: <0.001***, <0.01**, <0.05*.

displayed intermediate values with respect to the other two sites for AZ/VAZ and VA parameters (Table 3). In this sense, these results indicated a higher photoprotection status in PUCH plants than in those from BASE and PINGU.

Primary metabolism strongly differs between sites

A total of 69 metabolites were annotated and quantified in the leaves of DA (Supplementary Table S5). We first performed a sPLS-DA to compare the leaf metabolome depending on the different sites. The two major components explained 52.2% of the data variance (Fig. 4). PC1 (43.7%) separated PUCH plants from PINGU and BASE populations, while the PC2 (8.5%) separated plants from PINGU and BASE (Fig. 4). The major loadings for PC1 were related to N metabolism, osmoprotection, and polyamine synthesis, including serine, glutamate, proline,

Table 3. Photosynthetic pigment composition (mg g DW^{-1}) of *Deschampsia antarctica* plants in the three study sites (BASE, PINGU, and PUCH)

Site	Chl *a*	Chl *b*	Chl *a+b*	Neo	Viol	Ant	Lut	Zea	B-car	VA	VAZ
BASE	0.485 ± 0.020 a	0.121 ± 0.005 a	0.606 ± 0.026 a	0.024 ± 0.001 a	0.045 ± 0.002 a	0.012 ± 0.001 a	0.076 ± 0.003 a	0.019 ± 0.001 b	0.034 ± 0.001 a	0.057 ± 0.002 a	0.075 ± 0.002 a
PINGU	0.420 ± 0.030 ab	0.107 ± 0.009 ab	0.528 ± 0.039 ab	0.024 ± 0.003 ab	0.039 ± 0.004 ab	0.014 ± 0.002 a	0.068 ± 0.003 a	0.025 ± 0.005 b	0.030 ± 0.001 a	0.050 ± 0.003 ab	0.072 ± 0.002 a
PUCH	0.368 ± 0.039 b	0.088 ± 0.010 b	0.456 ± 0.049 b	0.018 ± 0.002 b	0.028 ± 0.003 b	0.014 ± 0.001 a	0.062 ± 0.005 a	0.036 ± 0.002 a	0.030 ± 0.002 a	0.042 ± 0.004 b	0.076 ± 0.007 a
F	4.41	4.75	4.49	4.50	8.61	0.58	3.26	14.16	1.61	7.07	0.14
***P*-value**	0.03*	0.02*	0.03*	0.03*	0.003**	0.57	0.06	<0.001***	0.23	<0.01**	0.87

The table also shows the *F* and *P*-values from one-way ANOVA. Neo, neoxanthin; Viol, violaxanthin; Ant, antheraxanthin; Lut, lutein; Zea, zeaxanthin; B-car, β-carotenes; V, violaxanthin; A, antheraxanthin; Z, zeaxanthin. Different letters indicate significant differences between sites by the multiple comparison Tukey's HSD test; *P*-value: <0.001***, <0.01**, <0.05*.

putrescine, and glutamine (Supplementary Fig. S6). The products of glutathione and ascorbate degradation (pyroglutamate and threonate, respectively) were higher in plants from BASE and PINGU than in those from PUCH. Interestingly, only one metabolite was relevant for the PC1, and was higher in PUCH plants than in those from the other sites: the non-reducing disaccharide trehalose, known to act as an osmoprotectant. PC2 explained a minor part of the variance and mainly separated plants from sites with enriched soils. The most important loadings in this component were intermediates of the tricarboxylic acid (TCA) cycle (citrate and succinate), lipid metabolism (glycerol-3P), S metabolism (*O*-acetyl-serine; OAS), secondary metabolism (3-caffeoylquinic acid; 3-CQA), and the hemicellulose component xylose (Supplementary Fig. S6).

A heatmap of the metabolites from plants growing at the different sites (Fig. 5) showed that PUCH plants had marked metabolic differences compared with plants from BASE and PINGU. The majority (58%) of the analyzed metabolites displayed significant changes; of these, 14 (20%) were increased and 26 (38%) were decreased. Differences between BASE and PINGU plants were less pronounced: only six metabolites were present at significantly different levels (9% of the analyzed metabolites), with an equal number of increased and reduced metabolites. In general, compared wuth PUCH plants, those from BASE and PINGU showed increased levels of compounds related to N metabolism, such as Glu, Gln, Asp, and Asn, as well as Pro and putrescine, which are known to act as osmoprotectants and cold tolerance drivers (Fig. 5). Strong, significant reductions were observed in BASE and PINGU plants for metabolites related to sugar metabolism (fructose, glucose, and maltose), particularly those related to membrane stabilization, such as trehalose and raffinose, as well as the precursors of raffinose synthesis, *myo*-inositol and galactinol (Fig. 5). Similarly, the precursors of lignin synthesis (*p*-coumarate, caffeate, and chlorogenate) and the products of cell wall degradation (galactose and xylose) were reduced in plants from BASE and PINGU (Fig. 5). The intermediates of the TCA cycle showed different patterns: citrate and fumarate were reduced and 2-oxoglutarate was increased in BASE and PINGU plants, whereas succinate and malate levels were similar in all studied sites (Fig. 5).

Discussion

Deschampsia antarctica plants show low genetic diversity but an important phenotypic plasticity in response to the environment, such as, for example, the soil nutrient availability along the maritime Antarctica (Smykla *et al.*, 2007; Chwedorzewska *et al.*, 2008; Park *et al.*, 2012, 2013; Holderegger *et al.*, 2018; Androsiuk *et al.*, 2021). In accordance, we observed contrasting vigor levels of DA in the surroundings of Henryk Arctowski Polish Antarctic Research Station (KGI, South Shetlands), depending on whether they were located in the tundra

Table 4. Photosynthetic pigment ratios of *Deschampsia antarctica* plants in the three studied sites (BASE, PINGU, and PUCH)

Site	Chl *a*/*b*	(AZ)/VAZ	B- car/Chl	VAZ/Chl	Neo/Chl	Vio/Chl	Ant/Chl	Lut/Chl	Zea/Chl
BASE	4.09 ± 0.03 ab	0.43 ± 0.01 b	93.81 ± 1.9 b	188.49 ± 4.7 b	59.81 ± 0.75 a	110.07 ± 2.7 a	33.12 ± 1.1 b	196.79 ± 3.0 a	50.176 ± 2.37 b
PINGU	4.01 ± 0.09 b	0.506 ± 0.05 b	93.0 ± 2.3 b	209.8 ± 18.7 b	61.03 ± 1.00 a	105.06 ± 3.6 ab	38.34 ± 5.3 ab	202.51 ± 9.1 a	70.82 ± 14.6 ab
PUCH	4.29 ± 0.05 a	0.63 ± 0.03 a	112.54 ± 4.2 a	249.79 ± 4.67 a	60.03 ± 0.41 a	93.43 ± 4.3 b	47.49 ± 3.2 a	215.80 ± 6.0 a	117.77 ± 11.61 a
F	5.06	13.14	8.15	11.67	0.68	6.33	6.06	3.12	14.78
***P*-value**	0.020*	<0.001***	0.003**	<0.001***	0.518	<0.01**	0.01*	0.07	>0.001***

The table shows the *F* and *P*-values from one-way ANOVA. Violaxanthin (V); antheraxanthin (A); zeaxanthin (Z); β-carotenes versus total chlorophyll ratio (B-car/Chl); violaxanthin plus antheraxanthin plus zeaxanthin versus total chlorophyll ratio (VAZ/Chl); neoxanthin versus total chlorophyll ratio (Neo/Chl); violaxanthin versus total chlorophyll ratio (Vio/Chl); antheraxanthin versus total chlorophyll ratio (Ant/Chl); lutein versus total chlorophyll ratio (Lut/Chl); zeaxanthin versus total chlorophyll ratio (Zea/Chl). Different letters indicate significant differences between sites by the multiple comparison Tukey´s HSD test; *P*-value: <0.001***, <0.01**, <0.05*.

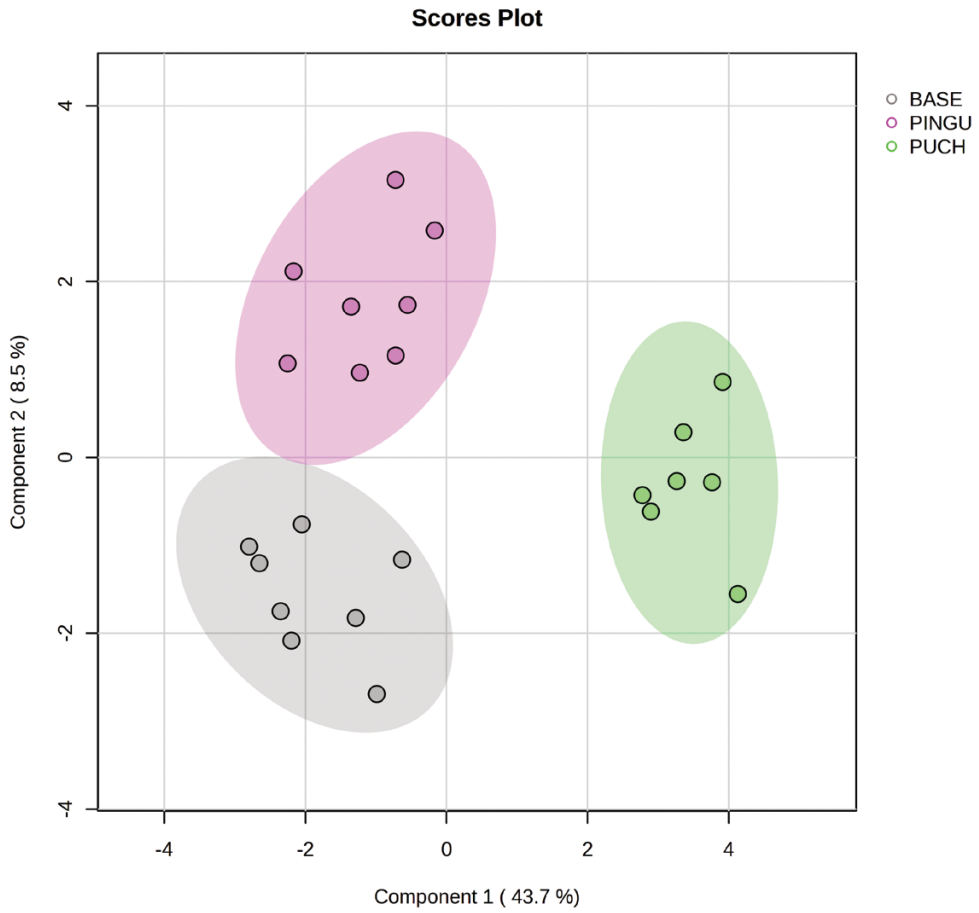

Fig. 4. Sparse partial least square discriminant analysis (sPLS-DA) of the metabolic profile of *Deschampsia antarctica* plants at the three different sites (BASE, PINGU, and PUCH) (*n*=6–8 individuals per site).

habitat (PUCH), close to the penguin rookeries (PINGU), or in human disturbed habitat, such as the buildings of the station (BASE). The photosynthetic performance, growth, and reproduction of several arctic and alpine tundra plant species are highly dependent on the availability of soil nutrients (Bowman *et al.*, 1993; Hobbie, 2007; Peterson, 2014; Körner, 2021). Experiments using nutrient addition (mostly N) in the arctic tundra have shown that, in general, grasses are the most responsive species, followed by forbs, deciduous shrubs, and evergreen shrubs (Shaver and Chapin, 1986; Chapin *et al.*, 1996). Moreover, increasing soil moisture in field experiments showed higher OM decomposition rates, significantly leading

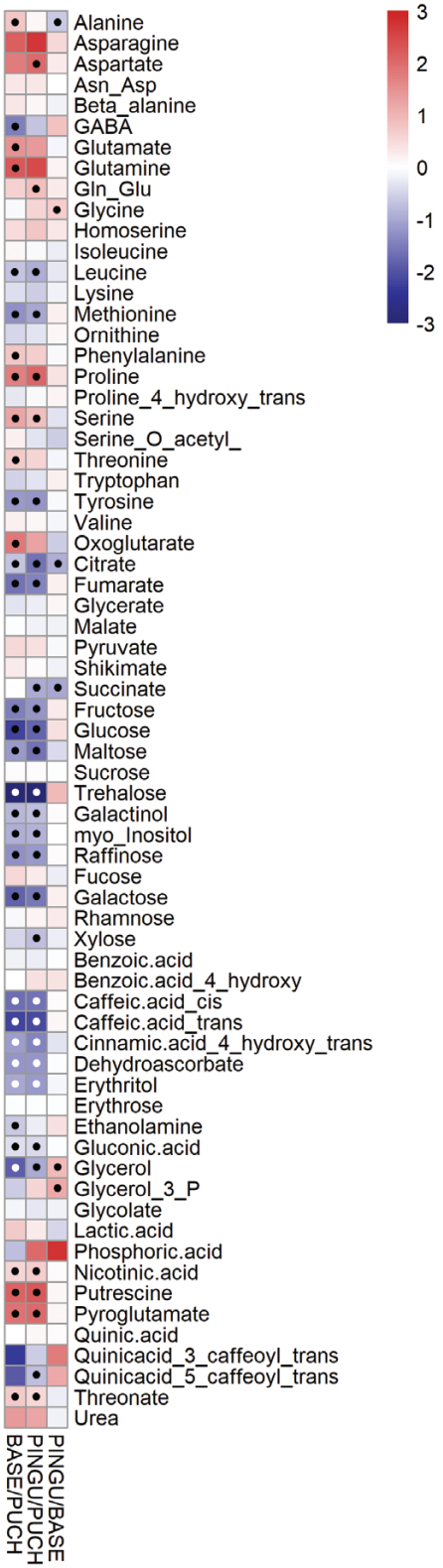

Fig. 5. Fold change heatmap of the leaf primary metabolism comparing *Deschampsia antarctica* plants at the tundra site (PUCH) with respect to the plants living in the surroundings of the base station (BASE) and penguin rookeries (PINGU). Dots indicate significant differences between the sites compared by Tukey's HSD test (P<0.05) (black dots) and (P<0.1) (white dots).

to higher nutrient availability, which in turn strongly affected the species community composition (Glanville *et al.*, 2012; Hicks Pries *et al.*, 2013; Semenchuk *et al.*, 2015; Scharn *et al.*, 2021).

However, to date, there are a limited number of molecular and ecophysiological studies dealing with plant species from extreme environments under field conditions; particularly those including the main photosynthetic physiological drivers (g_{sc}, g_m, and photobiochemistry) combined with primary metabolic profiling, as has been highlighted in recent reviews and meta-analyses (Dussarrat *et al.*, 2018; Fernández-Marín *et al.*, 2020; Knauer *et al.*, 2022). This topic remains relatively unexplored due to the inherent difficulties associated with working in these environments. Besides this, during the last decade, both vascular Antarctic species were the center of several ecophysiological works, mainly focused on their capacity for nutrient usage and association with endophyte funghi (Hill *et al.*, 2011, 2019; Park *et al.*, 2012, 2013; Rabert *et al.*, 2017; Santiago *et al.*, 2017). Additionally, their photosynthetic performances were thoroughly characterized by Sáez *et al.* (2017, 2018a, b), who showed that DA leaves displayed the anatomical traits typically observed in plants from xerophytic environments. Moreover, Rubisco kinetics showed significantly higher affinity for CO_2 under low temperature, in agreement with previous studies about the response of Rubisco activase to temperature (Salvucci *et al.*, 2004). Altogether, these data highlight the plasticity of DA for adapting to an extremely dry, cold, and nutrient-poor environment, but the main mechanisms coordinating photosynthetic capacity and stress tolerance under field conditions remain mostly unknown.

Interestingly, here we found that DA plants from sites differing in soil nutrient content showed no A_{area} differences and only marginal differences on a mass basis (P=0.096) (Table 1), although differences in the parameters limiting their photosynthesis were found (Table 2). These reduced differences in the carbon assimilation capacity, even for plants living in an extremely poor soil, could be explained by the previously described nutrient mobilization capacity from source to sink tissues, specifically in relation to N metabolism (Clemente-Moreno *et al.*, 2020). DA plants living in the tundra (PUCH) showed a significant physiological stress, whereas plants at BASE and PINGU (with higher availability of soil nutrients) were under optimal values (Table 1; Supplementary Table S4). Thus, despite similar levels of net carbon assimilation, central metabolism strongly differed between sites (Fig. 5), suggesting a differential molecular and physiological performance depending on the availability of soil nutrients, and not directly related to carbon resource limitations. In order to facilitate an integrative discussion, the major roles and physiological responses

of the main altered metabolic routes observed in this study are shown in Fig. 6.

The relationship of major nutrients, such as N and P, with the photobiochemistry and, subsequently, with the photosynthetic capacity, are well established in the literature (Walker *et al.*, 2014; Evans and Clarke, 2019; Knauer *et al.*, 2022), not only for model species but also for plants from extreme environments (Fernández-Marín *et al.*, 2020). It is thus surprising how DA, even in nutrient-limited soils (in terms of N or P), can still sustain substantial photosynthetic rates compared with species growing without nutrient limitations (Walker *et al.*, 2014; Gago *et al.*, 2019; Clemente-Moreno *et al.*, 2020). One possible explanation, however, is that DA possesses a highly efficient route for mobilizing N-rich metabolites from source to sink tissues when leaves cross a certain stress threshold, to be later employed when conditions again become favorable (Clemente-Moreno *et al.*, 2020).

The major photosynthetic limitation in DA from the nutrient-deprived soils was driven by g_m, being larger than that imposed by photobiochemistry (Table 2). How the availability of major nutrients affects g_m has seldom been addressed in the literature, which is surprising considering the multiple essential biochemical processes controlled by major nutrients in the leaf. For instance, g_m is frequently related to the activity of both aquaporins and carbonic anhydrases due to their roles in the transport of CO_2 through the membranes and through the cytosol and stroma, respectively. However, the mechanisms behind the relationship between N, P, and K, and g_m are still far from being completely understood (Xiong *et al.*, 2015; Barbour and Kaiser, 2016; Lundgren and Fleming, 2020; Evans, 2021; Knauer *et al.*, 2022).

Also, the cell wall is an important sink of C and N, and significantly contributes to the total cell dry mass (Onoda *et al.*, 2017). The higher LDMC shown by PUCH plants could be achieved through smaller cells and/or increased cell wall investment (Garnier and Laurent, 1994; Pyankov *et al.*, 1999; Castro-Díez *et al.*, 2000), ultimately affecting leaf functionality and its response to stress (Gago *et al.*, 2014, 2020). For instance, the proportion of their main components such as cellulose, hemicelluloses, pectins, lignin, phenols, and structural proteins would determine the size of the free spaces within the cell wall that the CO_2 needs to cross to reach the carboxylation sites in the chloroplast, thus affecting g_m and subsequently A_n (Ellsworth *et al.*, 2018; Clemente-Moreno *et al.*, 2019) in a mechanistic manner that is not fully understood yet (Gago *et al.*, 2020). Further, cell walls are dynamic structures that promptly respond to environmental changes, such as drought, where hydrophilic compounds, structural proteins, and lignification frequently increase to retain water and maintain the cell wall flexibility, to avoid the collapse by cell water losses (Moore *et al.*, 2013; Tenhaken, 2015). However, those changes have been suggested to decrease cell wall conductance to CO_2 due to the occlusion of pores and changes in its physico-chemical properties, interacting with the CO_2 diffusion pathway, reducing g_m and therefore A_n, and leading to ROS generation and oxidative stress (Monties, 1989; Niinemets *et al.*, 2009; Clemente-Moreno *et al.*, 2019; Flexas *et al.*, 2021). In addition, we observed changes in several mineral elements (e.g. Ca, B, and Cu, Supplementary Table S3) that are directly related to cell wall properties (Nari *et al.*, 1991; Fry *et al.*, 2002; Bascom *et al.*, 2018), and thus could be linked with cell wall composition and porosity, affecting g_m and the diffusive limitations imposed by the cell walls. In this sense, PUCH plants, compared with BASE and PINGU, showed a higher content of hydrophilic cell wall sugars such as as xylose (a major component of hemicelluloses) and galactose (mainly found in pectins), along with phenolic compounds such as *trans*-cinnamate and *p*-coumarate (Figs 5, 6), indicating significant cell wall remodeling, which in turn could sustain cell integrity but constrain g_m and photosynthetical capacity (Fig. 6).

A differential response of central metabolism: do what you can, with what you have, where you are

Overall, our results indicate that plants growing in a regular Antarctic tundra (PUCH), where the soil contains lower levels of macro- and micronutrients than in the other two sites, invest more carbon in compounds related to photoprotection such as carotenes and xanthophylls per chlorophyll, a higher activation of the VAZ cycle, protein and membrane stabilization, and structure remodeling (Table 4; Figs 5, 6). In this sense, a meta-analysis performed with 809 different species from green algae to mosses and vascular plants indicated that the VAZ cycle was highly responsive to the environment, including nutrient deficiency, showing the high phenotypic plasticity of VAZ driving photoprotection (Esteban *et al.*, 2015).

While PUCH plants drive their investments in direct efforts to provide photoprotection and structure stabilization, BASE and PINGU plants direct their metabolism to the synthesis of different amino acids, which is known to lead to the promotion of antioxidant activity and osmoprotection, besides their role as the building blocks for protein synthesis and thus growth promotion (Ishihara *et al.*, 2015, 2017; Li *et al.*, 2017; Duncan and Millar, 2022). BASE and PINGU plants showed lower levels of non-structural carbohydrates (glucose, fructose, maltose, raffinose, and trehalose) than those from PUCH (Figs 5, 6). The accumulation of trehalose and raffinose in PUCH plants could indicate a divergence in carbon metabolism to investments related to known stress tolerance responses. For instance, it is known that trehalose drives autophagy to remove cellular toxins, recycling of nutrients, and delaying senescence in the resurrection grass *Tripogon loliiformis* (Williams *et al.*, 2015), thus becoming an interesting biotechnological target for cereal improvement (Havé *et al.*, 2017).

Raffinose metabolism is universal in the plant kingdom and its accumulation has been implicated in cold tolerance and other abiotic stresses (Sengupta *et al.*, 2015). It has also been reported that raffinose is present in chloroplasts, where

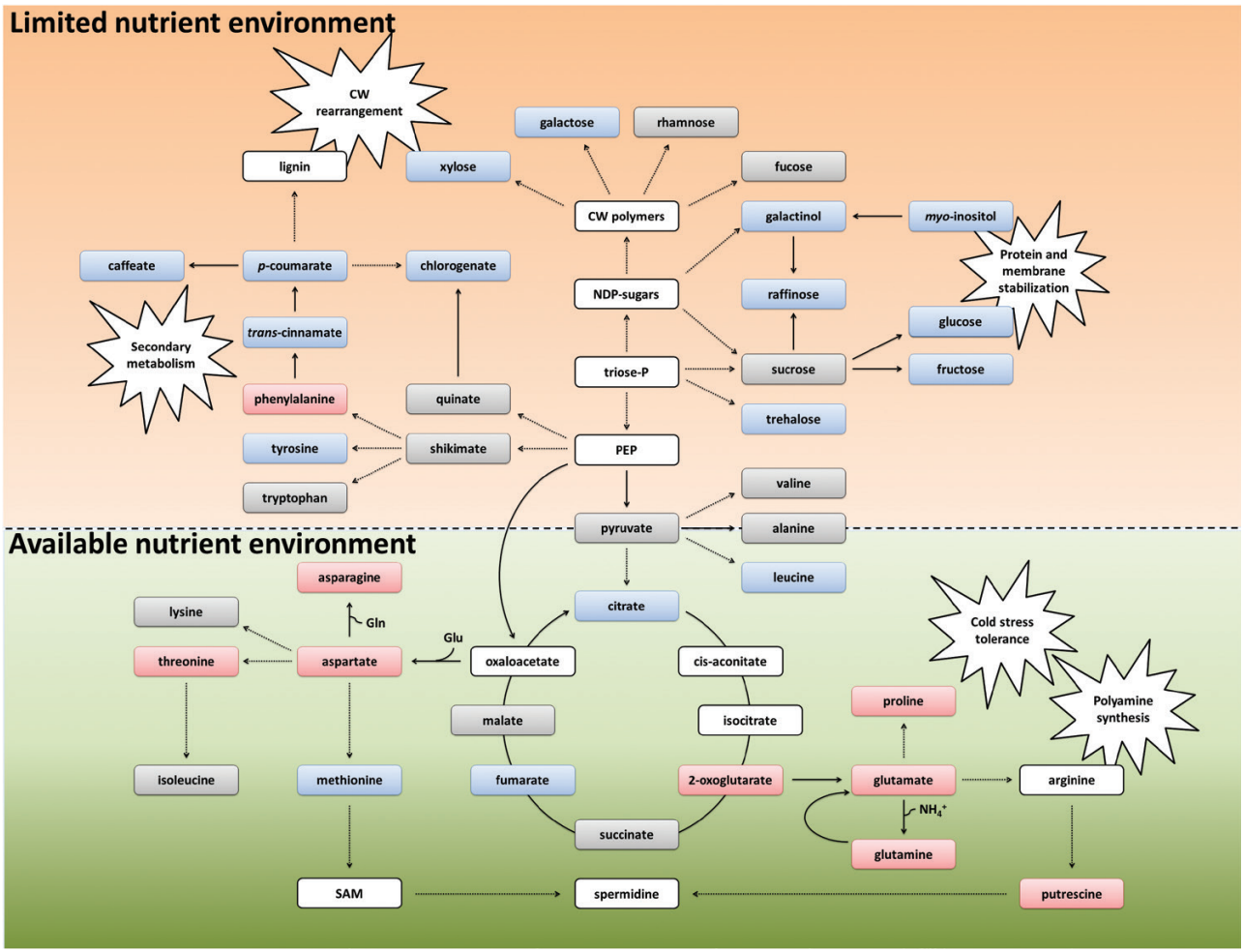

Fig. 6. Integrative metabolic pathway based into the relationship between BASE and PINGU plants (available nutrient environment) versus PUCH plants (limited nutrient environment). Boxes with blue and red colors indicate that metabolites are reduced or accumulated significantly comparing BASE/PINGU with respect to the PUCH metabolome. The orange and green shapes indicate the major metabolic pathways altered preferentially in the limited nutrient environment versus the available nutrient environment, respectively. Major roles and physiological responses of the main metabolic routes are indicated.

it could protect PSII during freeze–thaw cycles (Schneider and Keller, 2009; Knaupp *et al.*, 2011). In fact, the contents of certain amino acids (i.e. asparagine, aspartate, glutamine, and glutamate) were increased in BASE and PINGU plants compared with those from PUCH (Figs 5, 6). It seems that, due to the higher N availability in BASE and PINGU soils (Supplementary Table S1), plants growing in these sites divert more carbon to the synthesis of amino acids at the expense of sucrose synthesis, which may explain the reduced levels of soluble sugars (glucose, fructose, and raffinose) observed in these plants (Fig. 5) (Paul *et al.*, 1978; Larsen *et al.*, 1981). We consider that increased levels of these amino acids are not related to the reduction of protein synthesis by stress (Naidu *et al.*, 1991), as plants from BASE and PINGU were vigorous, actively growing, and without stress symptoms, as shown by the measured physiological indicators (Fig. 1; Table 1; Supplementary Table S4). Interestingly, such amino acids were previously reported to confer cold stress tolerance by lowering the levels of reducing equivalents through the malate–aspartate shuttle operating between plastids, mitochondria, and peroxisomes (Klotke *et al.*, 2004; Liepman and Olsen, 2004; Bocian *et al.*, 2015; Hoermiller *et al.*, 2017, and references therein) (Fig. 6).

DA plants can incorporate short peptides three times faster than free amino acids, nitrate, or ammonium as N source from the soils (Hill *et al.*, 2011). Moreover, Rabert *et al.* (2017) observed that DA plants showed higher biomass accumulation when fertilized with NH_4^+ rather than with NO_3^-, pointing to a preferential use of ammonium as N source. Thus, the relatively higher levels of aspartate, asparagine, glutamate, and glutamine in BASE and PINGU plants (Figs 5, 6) could be explained by the increased content of organic N and NH_4^+ in those locations.

It is important to note that aspartate and glutamate directly derive from TCA cycle intermediates (Fig. 6), and their synthesis ultimately depends on the available carbohydrate pools (Bocian *et al.*, 2015). In this sense, avoiding the accumulation

of carbohydrates by diverting carbon to the synthesis of these amino acids could prevent the feedback inhibition of photosynthesis by its own products (Lambers *et al.*, 2008; Bocian *et al.*, 2015). Moreover, such inhibition might be exacerbated in P-limited environments (as observed in PUCH, Fig. 3), where the accumulation of cytosolic phosphorylated intermediates could sequester the phosphate needed for the regeneration of the CBC intermediates (Groot *et al.*, 2003; Lambers *et al.*, 2008). This is in agreement with the results of the photosynthetic limitation analysis, where PUCH plants (which displayed higher levels of sugars than plants from the other two sites) were partially limited by biochemistry. Moreover, avoiding the feedback inhibition of photosynthesis by sugar accumulation also reduces photoinhibition and ROS production, and thus oxidative stress, by sustaining electron flow to the major sink of photosynthesis (Strand *et al.*, 1999; Distelbarth *et al.*, 2013), while accumulation of these amino acids ensures a valuable source of nitrogen and carbon skeletons to sustain plant performance in the harsh Antarctic environment.

Aspartate is the precursor of methionine, a key metabolite for the production of *S*-adenosylmethionine (SAM), which serves for multiple methylation reactions and the synthesis of ethylene, polyamines (such as spermidine and spermine), and the metal-chelating agent nicotianamine (Watanabe *et al.*, 2021). Glutamine and glutamate are essential not only for NH_4^+ fixation (Miflin and Habash, 2002), but also for the synthesis of other amino acids (such as aspartate and asparagine) and metabolites recognized to increase tolerance to low temperatures, such as proline and putrescine (the precursor of the polyamines spermidine and spermine) (Bocian *et al.*, 2015). All of them are significantly exacerbated in BASE plants compared with those from PUCH, indicating that these routes might play a major role driving their stress tolerance (Fig. 6).

Interestingly, the levels of both proline and putrescine in plants from BASE and PINGU were higher than in those from PUCH (Fig. 5). It has been described that proline has a double role as an osmolyte and anti-oxidant compound, thus driving low temperature stress tolerance (Smirnoff and Cumbes, 1989; Bravo *et al.*, 2001; Pérez-Torres *et al.*, 2007; Van den Ende, 2013; Fernández-Marín *et al.*, 2020). Similarly, polyamines are involved in numerous physiological processes, including stress tolerance. The levels of polyamines usually increase upon exposure to abiotic stress conditions. Moreover, overexpression of SAM decarboxylase (involved in polyamine biosynthesis) in economically important species (such as rice, tobacco, and tomato) increased the tolerance to various types of abiotic stress (Watanabe *et al.*, 2021).

The whole dataset indicates strong divergences in central metabolism, driven mainly by nutrient availability (Figs 4, 5). PUCH plants invest carbon in structural (cell wall and membrane) components and photoprotection, which could be related to the observed photosynthetical limitations imposed mostly by g_m and photobiochemistry, respectively. Conversely, PINGU and BASE plants seemed to invest carbon in amino acids (particularly proline) and polyamines (not only putrescine, but also spermidine and spermine), which might contribute to avoid oxidative stress when nutrients are available (Figs 5, 6). Among the different primary metabolic routes driving carbon to secondary metabolism, we only observed accumulation of phenylalanine in BASE and PINGU plants compared with PUCH (Fig. 5). This metabolite is the primary precursor of lignin, but also of several antioxidant secondary metabolites, such as phenylpropanoids and flavonoids (Tohge *et al.*, 2013). Thus, we speculate that carbon flux towards secondary antioxidant compounds via phenylalanine was increased in plants growing in BASE and PINGU compared with those from PUCH. Altogether, this could increase the antioxidant capacity while avoiding structural rearrangements, which in turn could constrain the CO_2 flow to the carboxylation sites in the chloroplast, and ultimately also the A_n (Fig. 6).

Conclusions

Overall, our results suggest that DA plants employ different photosynthetic and stress tolerance mechanisms depending on the soil nutrient availability. When nutrients are available, costly compounds in terms of mineral elements and energetic requirements (such as amino acids, secondary metabolites, and polyamines) are increased to keep oxidative stress under control. Conversely, plants growing in nutrient-limited environments (where N and P levels are considerably low) divert carbon to metabolites related to membrane, protein, and cell wall stabilization (such as raffinose, galactose, xylose trehalose, and *p*-coumarate, all of them cheaper compounds in terms of nutrients and ATP requirements), to avoid structure collapse under the higher levels of oxidative stress. These rearrangements could lead to the observed increased mesophyll and photobiochemical limitations. This response seems to be an attempt to sustain cell integrity at significant oxidative stress levels, when antioxidant (nutrient-costly) metabolism is constrained by the scarcity of resources.

Increases in temperature due to climate change in cold regions may increase nutrient cycling, generating more fertile soils for plant colonization (Chapin *et al.*, 1996). Global warming models for the AP and adjacent islands predict temperature increments and increases in the frequency and intensity of heat waves (Carrasco *et al.*, 2021; González-Herrero *et al.*, 2022). Warmer temperatures may facilitate nutrient cycling processes, therefore increasing their availability and allowing the subsequent proliferation of angiosperms (Hill *et al.*, 2019). Based on our results, namely the wide physiological and metabolic responses displayed by DA to nutrient availability, we hypothesize that this species could become more dominant in the terrestrial Antarctic communities under the predicted climatic change scenarios. This possible expansion of this species could be mediated by its differential employment of the available nutrients in osmoprotection and antioxidant capacity,

thus sustaining stress tolerance without penalizing their photosynthetical capacity.

Supplementary data

The following supplementary data are available at *JXB* online.

Fig. S1. *Deschampsia antarctica* leaf and air temperature 1 November 2017 to 1 May 2018 at Puchalski Hill, near Henryk Arctowski Polish Research Station in King George Island (South Shetlands).

Fig. S2. Major loadings from sPLS-DA showing the values of each element for component 1 and 2.

Fig. S3. Relationships between area-based net CO_2 assimilation (A_{area}) and the different estimated photosynthetic parameters across individuals from the different locations.

Fig. S4. Comparison of mesophyll conductance to CO_2 diffusion estimated from the variable J method ($g_{m\text{-}VJ}$) and the curve-fitting method ($g_{m\text{-}CF}$).

Fig. S5. Relationship between area-based net CO_2 assimilation (A_{area}) and CO_2 concentration inside chloroplasts estimated using the curve-fitting method ($C_{c\text{-}CF}$) from A–C_i curves.

Fig. S6. Major loadings from sPLS-DA showing the values of each metabolite for component 1 and 2.

Table S1. Soil fertility analysis from three different sites in the vicinity of the Henryk Arctowski Antarctic Research Polish Station.

Table S2. Soil ion content from the three different sites in the vicinity of the Henryk Arctowski Antarctic Research Polish Station.

Table S3. Leaf ion content from plants from the three different sites in the vicinity of the Henryk Arctowski Antarctic Research Polish Station.

Table S4. Pearson's correlation of F_v/F_m versus LMA, A_{mass}, A_{area}, ETR, P_r, g_{sc}, C_i, WUE_i, $g_{m\text{-}VJ}$, C_c, V_{cmax}, and J_{max} estimated using C_c, R_d, and NPQ.

Table S5. Average metabolite level ±SE (n=8) measured in the different sites.

Acknowledgements

The authors wish to publicly thank MCIN/AEI for the national research projects Proyectos I+D+i -Modalidades 'Retos Investigación' y 'Generación de Conocimiento' for 2015–2018 and 2019–2020. JG and JF are grateful to the national research project CTM2014-53902-C2-1-P funded by MCIN/AEI/10.13039/501100011033, and by 'ESF Investing in your future' and by 'European Union NextGenerationEU/PRTR'. MN was supported by the MINECO (Spain) and the European Social Fund (pre-doctoral fellowship BES-2015-072578), and acknowledges his postdoctoral contract Juan de la Cierva-Formación (FJC2020-043902-I), financed by MCIN/AEI/10.13039/501100011033 (Spain) and the European Union. MJC-M acknowledges her postdoctoral contract RYC2020-029602-I funded by MCIN/AEI/10.13039/501100011033. CMF is funded by the Max-Planck-Gesellschaft (Partner Group for Plant Biochemistry). LB and JG acknowledge financial support from FONDECYT (11130332; 1171640) and NEXER-UFRO (NXR17-002; Chile). MJC-M, LAC, LB, and JG also acknowledge REDES-CONICYT 170102 (Chile) for the Chile–Spain researcher exchange. LAC acknowledges funding from projects ACT210038 and FB21006. The authors also wish to thank the Instituto Antártico Chileno (INACH) for the support provided [including for the permits to sample the Antarctic base station Henryk Arctowski (Polska Akademia Nauk, Poland)], the ships *Lautaro* and *Aquiles* of the Armada de Chile (Chile) that make the work in Antarctica possible, and Dr Melanie Morales, who kindly provided pictures of *Deschampsia* turfs in King George Island close to Henryk Arctowski Antarctic Polish station.

Author contributions

MN, LB, and JGM: planning design; MN, LB, MJCM, DBM, NCR, and KL: performing the experiments, conducting fieldwork, and data analysis; MN, JG, JF, AF, CMF, MJCM, LAC, LB, and JGM: writing the manuscript.

Conflict of interest

The authors have no conflicts to declare.

Funding

This work was supported by the Ministerio de Ciencia, Innovación y Universidades (MCIN/AEI/10.13039/501100011033), by the Regional Development Fund (ERDF) 'A way of making Europe' [grant no. PGC2018-093824-B-C41], and MCIN/AEI/10.13039/501100011033 [grant no. PID2019-107434GA-I00].

Data availability

All data are available on request from the authors.

References

Androsiuk P, Chwedorzewska KJ, Dulska J, Milarska S, Giełwanowska I. 2021. Retrotransposon-based genetic diversity of *Deschampsia antarctica* Desv. from King George Island (Maritime Antarctic). Ecology and Evolution **11**, 648–663.

Angiel PJ, Potocki M, Biszczuk-Jakubowska J. 2010. Weather condition characteristics at the H. Arctowski Station (South Shetlands, Antarctica) for 2006, in comparison with multi-year research results. Miscellanea Geographica **14**, 79–89.

Barbour MM, Kaiser BN. 2016. The response of mesophyll conductance to nitrogen and water availability differs between wheat genotypes. Plant Science **251**, 119–127.

Bascom CS Jr, Hepler PK, Bezanilla M. 2018. Interplay between ions, the cytoskeleton, and cell wall properties during tip growth. Plant Physiology **176**, 28–40.

Beyer L, Bockheim JG, Campbell IB, Claridge GGC. 1999. Genesis, properties and sensitivity of Antarctic Gelisols. Antarctic Science **11**, 387–398.

Beyer M, Kühnhammer K, Dubbert M. 2020. In situ measurements of soil and plant water isotopes: a review of approaches, practical considerations and a vision for the future. Hydrology and Earth System Sciences **24**, 4413–4440.

Blume HP, Beyer L, Kalk E, Kuhn D. 2002. Weathering and soil formation. In: Beyer L, Bölter EM, eds. Geoecology of Antarctic ice free coastal landscapes. Berlin: Spinger-Verlag, 114–138.

Bocian A, Zwierzykowski Z, Rapacz M, Koczyk G, Ciesiołka D, Kosmala A. 2015. Metabolite profiling during cold acclimation of *Lolium perenne* genotypes distinct in the level of frost tolerance. Journal of Applied Genetics **56**, 439–449.

Bolter M. 2011. Soil development and soil biology on King George Island, maritime Antarctic. Polish Polar Research **32**, 105–116.

Bower CA, Wilcox LV. 1965. Soluble salts. In: Norman AG, ed. Methods of soil analysis: Part 2 chemical and microbiological properties. Chichester: Wiley, 933–951.

Bowman WD, Theodose TA, Schardt JC, Conant RT. 1993. Constraints of nutrient availability on primary production in two alpine tundra communities. Ecology **74**, 2085–2097.

Bravo LA, Ulloa N, Zuñiga GE, Casanova A, Corcuera LJ, Alberdi M. 2001. Cold resistance in antarctic angiosperms. Physiologia Plantarum **111**, 55–65.

Campbell IB, Claridge GGC. 1987. Antarctica: soils, weathering processes and environment. Amsterdam: Elsevier.

Carrasco JF, Bozkurt D, Cordero RR. 2021. A review of the observed air temperature in the Antarctic Peninsula. Did the warming trend come back after the early 21st hiatus? Polar Science **28**, 100653.

Casanova-Katny MA, Cavieres LA. 2012. Antarctic moss carpets facilitate growth of *Deschampsia antarctica* but not its survival. Polar Biology **35**, 1869–1878.

Castro-Díez P, Puyravaud JP, Cornelissen JHC. 2000. Leaf structure and anatomy as related to leaf mass per area variation in seedlings of a wide range of woody plant species and types. Oecologia **124**, 476–486.

Cavieres LA, Sáez P, Sanhueza C, Sierra-Almeida A, Rabert C, Corcuera LJ, Alberdi M, Bravo LA. 2016. Ecophysiological traits of Antarctic vascular plants: their importance in the responses to climate change. Plant Ecology **217**, 343–358.

Cavieres LA, Vivas M, Mihoc MA, Osses DA, Ortiz-Gutiérrez JM, Saéz PL, Bravo LA. 2018. The importance of facilitative interactions on the performance of *Colobanthus quitensis* in an Antarctic tundra. Journal of Vegetation Science **29**, 236–244.

Chapin IF, Bret-Harte MS, Hobbie SE, Zhong H. 1996. Plant functional types as predictors of transient responses of arctic vegetation to global change. Journal of Vegetation Science **7**, 347–358.

Chapman HD, Pratt PF. 1962. Methods of analysis for soils, plants and waters. Soil Science **93**, 68.

Chwedorzewska KJ, Giełwanowska I, Szczuka E, Bochenek A. 2008. High anatomical and low genetic diversity in *Deschampsia antarctica* Desv. from King George Island, the Antarctic. Polish Polar Research **29**, 377–386.

Clemente-Moreno MJ, Gago J, Díaz-Vivancos P, Bernal A, Miedes E, Bresta P, Flexas J. 2019. The apoplastic antioxidant system and altered cell wall dynamics influence mesophyll conductance and the rate of photosynthesis. The Plant Journal **99**, 1031–1046.

Clemente-Moreno MJ, Omranian N, Sáez PL, Figueroa CM, Del-Saz N, Elso M, Gago J. 2020. Low-temperature tolerance of the Antarctic species *Deschampsia antarctica*: a complex metabolic response associated with nutrient remobilization. Plant, Cell & Environment **43**, 1376–1393.

Convey P, Aitken S, Di Prisco G, *et al*. 2012. The impacts of climate change on circumpolar biodiversity. Biodiversity **13**, 134–143.

Convey P, Coulson SJ, Worland MR, Sjöblom A. 2018. The importance of understanding annual and shorter-term temperature patterns and variation in the surface levels of polar soils for terrestrial biota. Polar Biology **41**, 1587–1605.

Distelbarth H, Nägele T, Heyer AG. 2013. Responses of antioxidantenzymes to cold and high light are not correlated to freezing tolerance innatural accessions of *Arabidopsis thaliana*. Plant Biology **15**, 982–990.

Duncan O, Millar AH. 2022. Day and night isotope labelling reveal metabolic pathway specific regulation of protein synthesis rates in Arabidopsis. The Plant Journal **109**, 745–763.

Dussarrat T, Decros G, Díaz FP, Gibon Y, Latorre C, Rolin D, Gutiérrez RA, Pétriacq P. 2018. Another tale from the harsh world: how plants adapt to extreme environments. Annual Plant Reviews Online **4**, 551–603.

Edwards JA, Smith RI. 1988. Photosynthesis and respiration of *Colobanthus quitensis* and *Deschampsia antarctica* from the maritime Antarctic. British Antarctic Survey Bulletin **81**, 43–63.

Ellsworth PV, Ellsworth PZ, Koteyeva NK, Cousins AB. 2018. Cell wall properties in *Oryza sativa* influence mesophyll CO_2 conductance. New Phytologist **219**, 66–76.

Ensminger I, Busch F, Huner NP. 2006. Photostasis and cold acclimation: sensing low temperature through photosynthesis. Physiologia Plantarum **126**, 28–44.

Esteban R, Barrutia O, Artetxe U, Fernández-Marín B, Hernández A, García-Plazaola JI. 2015. Internal and external factors affecting photosynthetic pigment composition in plants: a meta-analytical approach. New Phytologist **206**, 268–280.

Evans JR. 2021. Mesophyll conductance: walls, membranes and spatial complexity. New Phytologist **229**, 1864–1876.

Evans JR, Clarke VC. 2019. The nitrogen cost of photosynthesis. Journal of Experimental Botany **70**, 7–15.

Farrer EC, Herman DJ, Franzova E, Pham T, Suding KN. 2013. Nitrogen deposition, plant carbon allocation, and soil microbes: changing interactions due to enrichment. American Journal of Botany **100**, 1458–1470.

Fernández-Marín B, Nadal M, Gago J, Fernie AR, López-Pozo M, Artetxe U, García-Plazaola JI, Verhoeven A. 2020. Born to revive: molecular and physiological mechanisms of double tolerance in a paleotropical and resurrection plant. New Phytologist **226**, 741–759.

Flexas J, Clemente-Moreno MJ, Bota J, *et al*. 2021. Cell wall thickness and composition are involved in photosynthetic limitation. Journal of Experimental Botany **72**, 3971–3986.

Flexas J, Díaz-Espejo A, Berry JA, Cifre J, Kaldenhoff R, Medrano H, Ribas-Carbó M. 2007. Analysis of leakage in IRGA's leaf chambers of open gas exchange systems: quantification and its effects in photosynthesis parameterization. Journal of Experimental Botany **56**, 1533–1543.

Fry SC, Miller JG, Dumville JC. 2002. A proposed role for copper ions in cell wall loosening. In: Horst WJ, Bürkert A, Claassen N, ***et al***., eds. Progress in plant nutrition: Plenary Lectures of the XIV International Plant Nutrition Colloquium. Dordrecht: Springer, 57–67.

Gago J, Douthe C, Florez-Sarasa I, Escalona JM, Galmes J, Fernie AR, Flexas J, Medrano H. 2014. Opportunities for improving leaf water use efficiency under climate change conditions. Plant Science **226**, 108–119.

Gago J, Carriquí M, Nadal M, Clemente-Moreno MJ, Coopman RE, Fernie AR, Flexas J. 2019. Photosynthesis optimized across land plant phylogeny. Trends in Plant Science **24**, 947–958.

Gago J, Daloso DM, Carriquí M, Nadal M, Morales M, Araújo WL, Nunes-Nesi A, Perera-Castro AV, Clemente-Moreno MJ, Flexas J. 2020. The photosynthesis game is in the'inter-play': mechanisms underlying CO_2 diffusion in leaves. Environmental and Experimental Botany **178**, 104–174.

Gallé A, Flórez-Sarasa I, El Aououad H, Flexas J. 2011. The Mediterranean evergreen *Quercus ilex* and the semi-deciduous *Cistus albidus* differ in their leaf gas exchange regulation and acclimation to repeated drought and re-watering cycles. Journal of Experimental Botany **62**, 5207–5216.

Garnier E, Laurent G. 1994. Leaf anatomy, specific mass and water content in congeneric annual and perennial grass species. New Phytologist **128**, 725–736.

Genty B, Briantais JM, Baker NR. 1989. The relationship between the quantum yield of photosynthetic electron transport and quenching of chlorophyll fluorescence. Biochimica et Biophysica Acta **990**, 87–92.

Glanville HC, Hill PW, Maccarone LD, Golyshin PN, Murphy DV, Jones DL. 2012. Temperature and water controls on vegetation emergence, microbial dynamics, and soil carbon and nitrogen fluxes in a high Arctic tundra ecosystem. Functional Ecology **26**, 1366–1380.

González-Herrero S, Barriopedro D, Trigo RM, López-Bustins JA, Oliva M. 2022. Climate warming amplified the 2020 record-breaking heatwave in the Antarctic Peninsula. Communications Earth & Environment **3**, 122.

Grassi G, Magnani F. 2005. Stomatal, mesophyll conductance and biochemical limitations to photosynthesis as affected by drought and leaf ontogeny in ash and oak trees. Plant, Cell & Environment **28**, 834–849.

Groot CC, Van Den Boogaard R, Marcelis LF, Harbinson J, Lambers H. 2003. Contrasting effects of N and P deprivation on the regulation of photosynthesis in tomato plants in relation to feedback limitation. Journal of Experimental Botany **54**, 1957–1967.

Harley PC, Loreto F, Di Marco G, Sharkey TD. 1992. Theoretical considerations when estimating the mesophyll conductance to CO_2 flux by analysis of the response of photosynthesis to CO_2. Plant Physiology **98**, 1429–1436.

Havé M, Marmagne A, Chardon F, Masclaux-Daubresse C. 2017. Nitrogen remobilization during leaf senescence: lessons from Arabidopsis to crops. Journal of Experimental Botany **68**, 2513–2529.

Hicks Pries CE, Schuur EAG, Vogel JG, Natali SM. 2013. Moisture drives surface decomposition in thawing tundra. Journal of Geophysical Research, Biogeosciences **118**, 1133–1143.

Hill PW, Farrar J, Roberts P, Farrell M, Grant H, Newsham KK, Hopkins DW, Bardgett RD, Jones DL. 2011. Vascular plant success in a warming Antarctic may be due to efficient nitrogen acquisition. Nature Climate Change **1**, 50–53.

Hill PW, Broughton R, Bougoure J, *et al*. 2019. Angiosperm symbioses with non-mycorrhizal fungal partners enhance N acquisition from ancient organic matter in a warming maritime Antarctic. Ecology Letters **22**, 2111–2119.

Hobbie SE, Ogdahl M, Chorover J, Chadwick OA, Oleksyn J, Zytkowiak R, Reich PB. 2007. Tree species effects on soil organic matter dynamics: the role of soil cation composition. Ecosystems **10**, 999–1018.

Hoermiller II, Naegele T, Augustin H, Stutz S, Weckwerth W, Heyer AG. 2017. Subcellular reprogramming of metabolism during cold acclimation in *Arabidopsis thaliana*. Plant, Cell & Environment **40**, 602–610.

Holderegger R, Stehlik I, Lewis Smith RI, Abbott RJ. 2018. Populations of Antarctic hairgrass (*Deschampsia antarctica*) show low genetic diversity. Arctic Antarctic and Alpine Research **35**, 214–217.

Hurry V, Strand A, Furbank R, Stitt M. 2000. The role of inorganic phosphate in the development of freezing tolerance and the acclimatization of photosynthesis to low temperature is revealed by the *pho* mutants of *Arabidopsis thaliana*. The Plant Journal **24**, 383–396.

Ishihara H, Moraes TA, Pyl ET, Schulze WX, Obata T, Scheffel A, Fernie AR, Sulpice R, Stitt M. 2017. Growth rate correlates negatively with protein turnover in Arabidopsis accessions. The Plant Journal **91**, 416–429.

Ishihara H, Obata T, Sulpice R, Fernie AR, Stitt M. 2015. Quantifying protein synthesis and degradation in Arabidopsis by dynamic $^{13}CO_2$ labeling and analysis of enrichment in individual amino acids in their free pools and in protein. Plant Physiology **168**, 74–93.

Jones ME, Bromwich DH, Nicolas JP, Carrasco J, Plavcová E, Zou X, Wang SH. 2019. Sixty years of widespread warming in the southern middle and high latitudes (1957–2016). Journal of Climate **32**, 6875–6898.

Klotke J, Kopka J, Gatzke N, Heyer AG. 2004. Impact of soluble sugar concentrations on the acquisition of freezing tolerance in accessions of *Arabidopsis thaliana* with contrasting cold adaptation—evidence for a role of raffinose in cold acclimation. Plant, Cell & Environment **27**, 1395–1404.

Knauer J, Cuntz M, Evans JR, Niinemets U, Tosens T, Veromann-Jürgenson LL, Werner C, Zaehle S. 2022. Contrasting anatomical and biochemical controls on mesophyll conductance across plant functional types. New Phytologist **236**, 357–368.

Knaupp M, Mishra KB, Nedbal L, Heyer AG. 2011. Evidence for a role of raffinose in stabilizing photosystem II during freeze–-thaw cycles. Planta **234**, 477–486.

Komárková V, Poncet S, Poncet J. 1985. Two native Antarctic vascular plants, *Deschampsia antarctica* and *Colobanthus quitensis*: a new southernmost locality and other localities in the Antarctic Peninsule area. Arctic and Alpine Research **17**, 401–416.

Kopka J, Schauer N, Krueger S, *et al*. 2005. GMD@CSB.DB: the Golm metabolome database. Bioinformatics **21**, 1635–1638.

Körner C. 2021. Alpine plant life: functional plant ecology of high mountain ecosystems. Berlin Heidelberg: Springer.

Kozeretska IA, Parnikoza IY, Mustafa O, Tyschenko OV, Korsun SG, Convey P. 2010. Development of Antarctic herb tundra vegetation near Arctowski station, King George Island. Polar Science **3**, 254–261.

Lambers H, Chapin FS, Pons TL. 2008. Plant physiological ecology, Vol. 2. New York: Springer.

Larsen PO, Cornwell KL, Gee SL, Bassham JA. 1981. Amino acid synthesis in photosynthesizing spinach cells: effects of ammonia on pool sizes and rates of labeling from $^{14}CO_2$. Plant Physiology **68**, 292–299.

Li L, Nelson CJ, Trösch J, Castleden I, Huang S, Millar AH. 2017. Protein degradation rate in *Arabidopsis thaliana* leaf growth and development. The Plant Cell **29**, 207–228.

Liepman AH, Olsen LJ. 2004. Genomic analysis of aminotransferases in *Arabidopsis thaliana*. Critical Reviews in Plant Sciences **23**, 73–89.

Lisec J, Schauer N, Kopka J, Willmitzer L, Fernie AR. 2006. Gas chromatography mass spectrometry-based metabolite profiling in plants. Nature Protocols **1**, 387–396.

Lundgren MR, Fleming AJ. 2020. Cellular perspectives for improving mesophyll conductance. The Plant Journal **101**, 845–857.

Maxwell K, Johnson GN. 2000. Chlorophyll fluorescence—a practical guide. Journal of Experimental Botany **51**, 659–668.

Mehlich A. 1984. Mehlich 3 soil test extractant: a modification of Mehlich 2 extractant. Communications in Soil Science and Plant Analysis **15**, 1409–1416.

Metson AJ. 1956. Methods of chemical analysis for soil survey samples. New Zealand Soil Bureau Bulletin 12. New Zealand Soil Bureau.

Miflin BJ, Habash DZ. 2002. The role of glutamine synthetase and glutamate dehydrogenase in nitrogen assimilation and possibilities for improvement in the nitrogen utilization of crops. Journal of Experimental Botany **53**, 979–987.

Monties B. 1989. Lignins. In: Harborne JB, ed. Methods in plant biochemistry, Vol. 1. London: Academic Press, 113–157.

Moore JP, Nguema-Ona EE, Vicre-Gibouin M, Sørensen I, Willats WG, Driouich A, Farrant JM. 2013. Arabinose-rich polymers as an evolutionary strategy to plasticize resurrection plant cell walls against desiccation. Planta **237**, 739–754.

Naidu BP, Paleg LG, Aspinall D, Jennings AC, Jones GP. 1991. Amino acid and glycine betaine accumulation in cold-stressed wheat seedlings. Phytochemistry **30**, 407–409.

Nari J, Noat G, Ricard J. 1991. Pectin methylesterase, metal ions and plant cell-wall extension. Hydrolysis of pectin by plant cell-wall pectin methylesterase. The Biochemical Journal **279**, 343–350.

Niinemets U, Cescatti A, Rodeghiero M, Tosens T. 2005. Leaf internal diffusion conductance limits photosynthesis more strongly in older leaves of Mediterranean evergreen broad-leaved species. Plant, Cell & Environment **28**, 1552–1566.

Niinemets U, Díaz-Espejo A, Flexas J, Galmés J, Warren CR. 2009. Role of mesophyll diffusion conductance in constraining potential photosynthetic productivity in the field. Journal of Experimental Botany **60**, 2249–2270.

Onoda Y, Wright IJ, Evans JR, Hikosaka K, Kitajima K, Niinemets U, Poorter H, Tosens T, Westoby M. 2017. Physiological and structural tradeoffs underlying the leaf economics spectrum. New Phytologist **214**, 1447–1463.

Park JS, Ahn IY, Lee EJ. 2012. Influence of soil properties on the distribution of *Deschampsia antarctica* on King George Island, Maritime Antarctica. Polar Biology **35**, 1703–1711.

Park JS, Ahn IY, Lee EJ. 2013. Spatial distribution patterns of the Antarctic hair grass *Deschampsia antarctica* in relation to environmental variables on

Barton Peninsula, King George Island. Arctic Antarctic and Alpine Research **45**, 563–574.

Paul F, Coulet PR, Gautheron DC, Engasser JM. 1978. Kinetics of collagen-bound sorbitol dehydrogenase in the rotating membrane reactor: opposite variations of affinity constants under diffusional limitations. Biotechnology and Bioengineering **20**, 1785–1796.

Peat HJ, Clarke A, Convey P. 2007. Diversity and biogeography of the Antarctic flora. Journal of Biogeography **34**, 132–146.

Pérez-Torres E, Bravo LA, Corcuera LJ, Johnson GN. 2007. Is electron transport to oxygen an important mechanism in photoprotection? Contrasting responses from Antarctic vascular plants. Physiologia Plantarum **130**, 185–194.

Pérez-Torres E, Dinamarca J, Bravo LA, Corcuera LJ. 2004a. Responses of *Colobanthus quitensis* (Kunth) Bartl. to high light and low temperature. Polar Biology **27**, 183–189.

Pérez-Torres E, García A, Dinamarca J, Alberdi M, Gutiérrez A, Gidekel M, Ivanov AG, Hüner NPA, Corcuera LJ, Bravo LA. 2004b. The role of photochemical quenching and antioxidants in photoprotection of *Deschampsia antarctica*. Functional Plant Biology **31**, 731–741.

Peterson KM. 2014. Plants in Arctic environments. In: Monson R, ed. Ecology and the environment. The plant sciences, vol. 8. New York: Springer, 363–388.

Pons TL, Flexas J, von Caemmerer S, Evans JR, Genty B, Ribas-Carbó M, Brugnoli E. 2009. Estimating mesophyll conductance to CO_2: methodology, potential errors, and recommendations. Journal of Experimental Botany **60**, 2217–2234.

Pyankov V, Kondratchuk AV, Shipley B. 1999. Leaf structure and specific leaf mass: the alpine desert plants of the Eastern Pamirs, Tadjikistan. New Phytologist **143**, 131–142.

Rabert C, Reyes-Díaz M, Corcuera LJ, Bravo LA, Alberdi M. 2017. Contrasting nitrogen use efficiency of Antarctic vascular plants may explain their population expansion in Antarctica. Polar Biology **40**, 1569–1580.

Sáez PL, Bravo LA, Cavieres LA, Vallejos V, Sanhueza C, Font-Carrascosa M, Gil-Pelegrín E, Peguero-Pina JJ, Galmés J. 2017. Photosynthetic limitations in two Antarctic vascular plants: importance of leaf anatomical traits and Rubisco kinetic parameters. Journal of Experimental Botany **68**, 2871–2883.

Sáez PL, Bravo LA, Latsague MI, Toneatti MJ, Sánchez-Olate M, Ríos DG. 2013. Light energy management in micropropagated plants of *Castanea sativa*, effects of photoinhibition. Plant Science **201**, 12–24.

Sáez PL, Cavieres LA, Galmés J, *et al*. 2018a. In situ warming in the Antarctic: effects on growth and photosynthesis in Antarctic vascular plants. New Phytologist **218**, 1406–1418.

Sáez PL, Galmés J, Ramírez CF, Poblete L, Rivera BK, Cavieres LA, Clemente-Moreno MJ, Flexas J, Bravo LA. 2018b. Mesophyll conductance to CO_2 is the most significant limitation to photosynthesis at different temperatures and water availabilities in Antarctic vascular species. Environmental and Experimental Botany **156**, 279–287.

Salvucci ME, Crafts-Brandner SJ. 2004. Relationship between the heat tolerance of photosynthesis and the thermal stability of Rubisco activase in plants from contrasting thermal environments. Plant Physiology **134**, 1460–1470.

Santiago IF, Rosa CA, Rosa LH. 2017. Endophytic symbiont yeasts associated with the Antarctic angiosperms *Deschampsia antarctica* and *Colobanthus quitensis*. Polar Biology **40**, 177–183.

Scharn R, Little CJ, Bacon CD, Alatalo JM, Antonelli A, Björkman MP, Molau U, Nilson RH, Björk RG. 2021. Decreased soil moisture due to warming drives phylogenetic diversity and community transitions in the tundra. Environmental Research Letters **16**, 064031.

Schimel JP, Kielland K, Chapin FS. 1996. Nutrient availability and uptake by tundra plants. In: Reynolds JF, Tenhunen JD, eds. Landscape function and disturbance in arctic tundra. Berlin, Heidelberg: Springer, 203–221.

Schneider T, Keller F. 2009. Raffinose in chloroplasts is synthesized in the cytosol and transported across the chloroplast envelope. Plant and Cell Physiology **50**, 2174–2182.

Semenchuk PR, Elberling B, Amtorp C, Winkler J, Rumpf S, Michelsen A, Cooper EJ. 2015. Deeper snow alters soil nutrient availability and leaf nutrient status in high Arctic tundra. Biogeochemistry **124**, 81–94.

Sengupta S, Mukherjee S, Basak P, Majumder AL. 2015. Significance of galactinol and raffinose family oligosaccharide synthesis in plants. Frontiers in Plant Science **6**, 656.

Sharkey TD. 2016. What gas exchange data can tell us about photosynthesis. Plant, Cell & Environment **39**, 1161–1163.

Sharkey TD, Bernacchi CJ, Farquhar GD, Singsaas EL. 2007. Fitting photosynthetic carbon dioxide response curves for C_3 leaves. Plant, Cell & Environment **30**, 1035–1040.

Shaver GR, Chapin IF. 1986. Effect of fertilizer on production and biomass of tussock tundra, Alaska, USA. Arctic and Alpine Research **18**, 261–268.

Smirnoff N, Cumbes QJ. 1989. Hydroxyl radical scavenging activity of compatible solutes. Phytochemistry **28**, 1057–1060.

Smith R. 2003. The enigma of *Colobanthus quitensis* and *Deschampsia antarctica* in Antarctica. In: Huiskes AHL, Gieskes WWC, Rozema J, Schorno RML, van der Vies SM, Wolff WJ, eds. Antarctic biology in a global context. Leiden: Backhuys, 234–239.

Smykla J, Wołek J, Barcikowski A. 2007. Zonation of vegetation related to penguin rookeries on King George Island, Maritime Antarctic. Arctic Antarctic and Alpine Research **39**, 143–151.

Strand A, Hurry V, Henkes S, Huner N, Gustafsson P, Gardeström P, Stitt M. 1999. Acclimation of Arabidopsis leaves developing at low temperatures. Increasing cytoplasmic volume accompanies increased activities of enzymes in the Calvin cycle and in the sucrose-biosynthesis pathway. Plant Physiology **119**, 1387–1398.

Tenhaken R. 2015. Cell wall remodeling under abiotic stress. Frontiers in Plant Science **5**, 771.

Tohge T, Watanabe M, Hoefgen R, Fernie AR. 2013. Shikimate and phenylalanine biosynthesis in the green lineage. Frontiers in Plant Science **4**, 62.

Turner J, Lu H, White I, King JC, Phillips T, Hosking JS, Bracegirdle TJ, Marshall GJ, Mulvaney R, Deb P. 2016. Absence of 21st century warming on Antarctic Peninsula consistent with natural variability. Nature **535**, 411–415.

Vaieretti MV, Díaz S, Vile D, Garnier E. 2007. Two measurement methods of leaf dry matter content produce similar results in a broad range of species. Annals of Botany **99**, 955–958.

Valentini R, Epron D, De Angelis P, Matteucci G, Dreyer E. 1995. In situ estimation of net CO_2 assimilation, photosynthetic electron flow and photorespiration in Turkey oak (*Q. cerris* L.) leaves: diurnal cycles under different levels of water supply. Plant, Cell & Environment **18**, 631–640.

Van den Ende W. 2013. Multifunctional fructans and raffinose family oligosaccharides. Frontiers in Plant Science **4**, 247.

Walker RT, Parizek BR, Alley RB, Brunt KM, Anandakrishnan S. 2014. Ice-shelf flexure and tidal forcing of Bindschadler Ice Stream, West Antarctica. Earth and Planetary Science Letters **395**, 184–193.

Wasley J, Robinson SA, Lovelock CE, Popp M. 2006. Climate change manipulations show Antarctic flora is more strongly affected by elevated nutrients than water. Global Change Biology **12**, 1800–1812.

Watanabe M, Chiba Y, Hirai MY. 2021. Metabolism and regulatory functions of O-acetylserine, S-adenosylmethionine, homocysteine, and serine in plant development and environmental responses. Frontiers in Plant Science **12**, 593.

Williams B, Njaci I, Moghaddam L, Long H, Dickman MB, Zhang X, Mundree S. 2015. Trehalose accumulation triggers autophagy during plant desiccation. PLoS Genetics **11**, e1005705.

Xiong D, Liu XI, Liu L, Douthe C, Li Y, Peng S, Huang J. 2015. Rapid responses of mesophyll conductance to changes of CO_2 concentration, temperature and irradiance are affected by N supplements in rice. Plant, Cell & Environment **38**, 2541–2550.

Xiong FS, Ruhland CT, Day TA. 1999. Photosynthetic temperature response of the Antarctic vascular plants *Colobanthus quitensis* and *Deschampsia antarctic*a. Physiologia Plantarum **106**, 276–286.